

Conservative and dissipative discretisations of multi-conservative ODEs and GENERIC systems

Boris D. Andrews^a, Patrick E. Farrell^{a,b}

^a*Mathematical Institute, University of Oxford, UK*

^b*Mathematical Institute, Faculty of Mathematics and Physics, Charles University, Czechia*

Abstract

Partial differential equations (PDEs) describing thermodynamically isolated systems typically possess conserved quantities (like mass, momentum, and energy) and dissipated quantities (like entropy). Preserving these conservation and dissipation laws on discretisation in time can yield vastly better approximations for the same computational effort, compared to schemes that are not structure-preserving. In this work we present two novel contributions: (i) an arbitrary-order time discretisation for general conservative ordinary differential equations that conserves all known invariants and (ii) an energy-conserving and entropy-dissipating scheme for both ordinary and partial differential equations written in the GENERIC format, a superset of Poisson and gradient-descent systems. In both cases the underlying strategy is the same: the systematic introduction of auxiliary variables, allowing for the replication at the discrete level of the proofs of conservation or dissipation. We illustrate the advantages of our approximations with numerical examples of the Kepler and Kovalevskaya problems, a combustion engine model, and the Benjamin–Bona–Mahony equation.

Keywords: geometric numerical integration, structure preservation, conservation laws, dissipation inequalities

2000 MSC: 65M60, 37K99, 37L99

1. Introduction

Preserving geometric structure on discretisation has emerged as one of the key themes in modern numerical analysis. For initial-value problems (IVPs) on ordinary (ODEs) and partial (PDEs) differential equations, desirable features include symplecticity, reversibility, contractivity, maximum principles, nonnegativity, conservation laws, and dissipation inequalities. The art of designing such structure-preserving integrators is known as geometric numerical integration [1]. In general, it is not possible to preserve every such feature simultaneously; for example, the celebrated Ge–Marsden theorem shows that approximate symplectic algorithms cannot conserve energy for certain nonintegrable Hamiltonian systems [2]. To faithfully reproduce the characteristics of a problem’s exact solution at the discrete level, one should target those structures that are most influential in the behaviour of the solution.

In this work, we further develop a framework recently proposed by the authors [3] for devising time discretisations that exactly reproduce (up to machine precision, solver tolerances, and quadrature errors) conservation laws and dissipation inequalities. We extend the ideas of [3] in two directions. For general conservative ODEs, we construct arbitrary-order integrators that exactly conserve all invariants. For ODEs and PDEs written in the GENERIC (General Equation for Non-Equilibrium Reversible-Irreversible Coupling) formalism [4, 5], an abstract thermodynamically-compatible expression of certain IVPs, we obtain schemes that simultaneously conserve energy and dissipate entropy. We also present numerical examples where preserving these structures appears to offer decisive advantages over typical methods (e.g. those preserving symplecticity) for single simulations over relatively long timescales. As in our prior work [3], the unifying idea is the use of *auxiliary variables*, i.e. projections of certain *associated test functions* (e.g. gradients of these quantities of interest in the ODE case) onto a discrete test space.

Both contributions we present are novel. For conservative ODEs, the most closely related works include those of Cohen & Hairer [6] (considering the conservation of a single invariant) and of Brugnano, Iavernaro & Frasca-Caccia [7, 8, 9] (in the multiply conservative case); in contrast to our approach, the scheme of Brugnano *et al.* requires the use of at least as many stages as conservation laws to be preserved. The discretisation we propose for GENERIC systems

generalises the works of Romero [10] (in the case of ODEs at lowest order in time) and of Giesselmann, Karsai & Tscherpel [11] (when applied to Poisson or gradient-descent PDEs).

The remainder of this manuscript proceeds as follows. In Section 2, we develop the conservative ODE integrator; we illustrate its structure-preserving properties with numerical demonstrations on the Kepler and Kovalevskaya problems. In Section 3, we present the GENERIC ODE construction, with a similar numerical example on an unfired combustion engine. In Section 4, we extend this idea to GENERIC PDEs; to demonstrate our construction, we consider the Boltzmann and Benjamin–Bona–Mahony equations, with numerical demonstration of the latter. We offer some concluding remarks in Section 5.

2. General conservative ODEs

We first consider general conservative ODE systems with possibly many invariants. Let $\mathbf{f} : \mathbb{R}^d \rightarrow \mathbb{R}^d$ induce the general ODE system

$$\dot{\mathbf{x}} = \mathbf{f}(\mathbf{x}), \quad (1)$$

with initial condition (IC) $\mathbf{x}(0) = \mathbf{x}_0$. Suppose this system is conservative in $P (< d)$ independent invariants ($N_p : \mathbb{R}^d \rightarrow \mathbb{R}$) $_{p=1}^P$, with the property that $\nabla N_p(\mathbf{x})^\top \mathbf{f}(\mathbf{x}) = 0$ for each $p = 1, \dots, P$. Each N_p can then be seen to be conserved over a timestep $T_n := [t_n, t_{n+1}]$ by testing (1) with ∇N_p :

$$N_p(x_{n+1}) - N_p(x_n) = \int_{T_n} \dot{N}_p = \int_{T_n} \nabla N_p(\mathbf{x}) \cdot \dot{\mathbf{x}} = \int_{T_n} \nabla N_p(\mathbf{x})^\top \mathbf{f}(\mathbf{x}) = 0. \quad (2)$$

Before considering the general system (1) in further detail, it is instructive to consider a Poisson system,

$$\mathbf{f}(\mathbf{x}) = B(\mathbf{x})\nabla H(\mathbf{x}), \quad (3)$$

where $B(\mathbf{x}) \in \mathbb{R}^{d \times d}$ is a skew-symmetric matrix encoding the Poisson bracket, and H is the conserved Hamiltonian¹. In this case, the relation $\nabla H(\mathbf{x})^\top \mathbf{f}(\mathbf{x}) = \nabla H(\mathbf{x})^\top B(\mathbf{x})\nabla H(\mathbf{x}) = 0$ follows from the skew-symmetry of B . A broad class of discretisations for (3) is of the form: find $\mathbf{x} \in \mathbb{X}_n$ such that

$$\mathcal{I}_n [\mathbf{y}^\top \dot{\mathbf{x}}] = \mathcal{I}_n [\mathbf{y}^\top B(\mathbf{x})\nabla H(\mathbf{x})] \quad (4)$$

for all $\mathbf{y} \in \mathbb{X}_n$. Here \mathbb{X}_n is the trial space of polynomials of a fixed degree $s \geq 1$ satisfying known initial data at the beginning of the timestep,

$$\mathbb{X}_n := \left\{ \mathbf{y} \in \mathbb{P}_s(T_n; \mathbb{R}^d) \mid \mathbf{y}(t_n) \text{ satisfies known initial data} \right\}, \quad (5)$$

with its time derivative satisfying $\dot{\mathbb{X}}_n = \mathbb{P}_{s-1}(T_n; \mathbb{R}^d)$. The operator \mathcal{I}_n is a linear approximation to the integral over T_n (a quadrature rule), i.e. $\mathcal{I}_n[\phi] \approx \int_{T_n} \phi$, specifying the time discretisation; the approximation must be sign-preserving, i.e.

$$\phi \geq 0 \implies \mathcal{I}_n[\phi] \geq 0, \quad (6a)$$

appropriately scaled in $\Delta t_n := t_{n+1} - t_n$, i.e.

$$\mathcal{I}_n[1] = \Delta t_n, \quad (6b)$$

and the map $\phi \mapsto \mathcal{I}_n[\phi^2]^{\frac{1}{2}}$ must define a norm on $\mathbb{P}_{s-1}(T_n)$. Examples of such linear operators include any $\geq s$ -stage quadrature rule with positive weights, and the exact integral. In the case where \mathcal{I}_n is an s -stage quadrature rule, (4) is equivalent to a collocation method at the quadrature points (see [12, Sec. II.1.2]); in the case where \mathcal{I}_n is the exact integral, (4) is a continuous Petrov–Galerkin discretisation in time (see [13, Chap. 70]).

We wish to discretise (3) in time while retaining the conservation of H . However, the time discretisation (4) cannot in general achieve this. The central difficulty with reproducing the conservation argument for the continuous case is

¹Since we do not impose the Jacobi identity on B , this would more precisely be referred to as *almost* Poisson. However, we use the former terminology throughout this manuscript for brevity.

that $\nabla H(\mathbf{x}) \notin \mathbb{X}_n$, i.e. $\nabla H(\mathbf{x})$ is not a valid choice of discrete test function. This may be overcome by introducing an auxiliary variable $\widetilde{\nabla H} \in \mathbb{X}_n$ approximating $\nabla H(\mathbf{x})$, yielding the scheme: find $(\mathbf{x}, \widetilde{\nabla H}) \in \mathbb{X}_n \times \mathbb{X}_n$ such that

$$\mathcal{I}_n[\mathbf{y}^\top \dot{\mathbf{x}}] = \mathcal{I}_n[\mathbf{y}^\top B(\mathbf{x}) \widetilde{\nabla H}], \quad (7a)$$

$$\mathcal{I}_n[\widetilde{\nabla H}^\top \mathbf{y}_0] = \int_{T_n} \nabla H(\mathbf{x})^\top \mathbf{y}_0, \quad (7b)$$

for all $(\mathbf{y}, \mathbf{y}_0) \in \mathbb{X}_n \times \mathbb{X}_n$.

Proposition 2.1 (Conservation properties of (7)). *Assuming solutions exist, the integrator (7) satisfies $H(\mathbf{x}(t_{n+1})) = H(\mathbf{x}(t_n))$ (up to quadrature errors, solver tolerances, and machine precision) at every timestep.*

Proof. Mimicking the continuous argument, we consider respectively $\mathbf{y}_0 = \dot{\mathbf{x}}$ in (7b) and $\mathbf{y} = \widetilde{\nabla H}$ in (7a):

$$H(\mathbf{x}(t_{n+1})) - H(\mathbf{x}(t_n)) = \int_{T_n} \dot{H} = \int_{T_n} \nabla H(\mathbf{x})^\top \dot{\mathbf{x}} = \mathcal{I}_n[\widetilde{\nabla H}^\top \dot{\mathbf{x}}] = \mathcal{I}_n[\widetilde{\nabla H}^\top B(\mathbf{x}) \widetilde{\nabla H}] = 0. \quad (8)$$

□

Summarising the strategy in the construction of (7), we (i) introduce an *auxiliary variable* corresponding to the quantity we wish to preserve, namely a projection of its gradient onto the discrete test space \mathbb{X}_n , and (ii) modify the right-hand side to use the auxiliary variable so that the conservation proof can be replicated discretely. In the context of [3], the gradient ∇H is the *associated test function* corresponding to H ; namely, it is the function against which one would test the equation (3) to derive the conservation or dissipation law in the continuous setting, and consequently that which we introduce into our discretisation through a discrete auxiliary variable to preserve that law.

Remark 2.2. *In practice, the scheme (7) incurs little additional computational cost over (4) as the auxiliary variable $\widetilde{\nabla H}$ can be evaluated explicitly. In the case of \mathcal{I}_n an s -stage quadrature rule, the resulting reformulation can then be shown to be equivalent to the scheme of Cohen & Hairer [6], which is in turn at lowest order in time equivalent to the mean-value discrete-gradient method of McLachlan, Quispel & Robidoux [14]. However, our interpretation extends more easily to the conservation of additional invariants, alongside the consideration of PDEs wherein these auxiliary variables cannot in general be evaluated explicitly.*

We now return to the general case (1). The same strategy suggests (i) introducing auxiliary variables $\{\widetilde{\nabla N}_p\}$ approximating each $\nabla N_p(\mathbf{x})$, and (ii) using these new variables in the right-hand side of (1), as done in (7). However, as written, (1) does not appear to depend on $\{\nabla N_p\}$. The following theorem demonstrates that in fact \mathbf{f} may be rewritten to expose an explicit dependence on $\{\nabla N_p\}$, thereby enabling the incorporation of the auxiliary variables $\{\widetilde{\nabla N}_p\}$. This result is fully constructive. In particular, we rewrite \mathbf{f} in terms of an alternating form, i.e. a multilinear map $F : V^n \rightarrow \mathbb{R}$ over a vector space V such that $F[v_1, \dots, v_n] = 0$ whenever $v_i = v_j$ for some $i \neq j$. We denote the space of alternating n -forms over V by $\text{Alt}^n V$, and define the alternatisation $\text{Alt } F \in \text{Alt}^n V$ of an n -multilinear map by

$$\text{Alt } F[v_1, \dots, v_n] := \sum_{\sigma \in S_n} \text{sgn}_\sigma F[v_{\sigma_1}, \dots, v_{\sigma_n}], \quad (9)$$

where S_n denotes the permutation group of degree n , and $\text{sgn}_\sigma \in \{\pm 1\}$ the sign of $\sigma \in S_n$ [15].

Theorem 2.3 (Identification of alternating forms). *For the general conservative system (1) there exists $\tilde{F} : \mathbb{R}^d \rightarrow \text{Alt}^{P+1} \mathbb{R}^d$ such that $\forall \mathbf{x}, \mathbf{y} \in \mathbb{R}^d$,*

$$\mathbf{y}^\top \mathbf{f}(\mathbf{x}) = \tilde{F}(\mathbf{x})[\nabla N_1(\mathbf{x}), \dots, \nabla N_P(\mathbf{x}), \mathbf{y}]. \quad (10)$$

Proof. We demonstrate the existence of \tilde{F} by construction. Through the independence of (N_p) , the gradients (∇N_p) are linearly independent almost everywhere. Consequently, we may define a dual basis $(\mathbf{m}_q : \mathbb{R}^d \rightarrow \mathbb{R}^d)_{q=1}^P$ such that almost everywhere $\nabla N_p(\mathbf{x})^\top \mathbf{m}_q(\mathbf{x}) = \delta_{pq}$. For each $\mathbf{x} \in \mathbb{R}^d$, define the multilinear map $\tilde{G}(\mathbf{x}) : (\mathbb{R}^d)^{P+1} \rightarrow \mathbb{R}$,

$$\tilde{G}(\mathbf{x})[\mathbf{n}_1, \dots, \mathbf{n}_P, \mathbf{y}] := (\mathbf{n}_1^\top \mathbf{m}_1(\mathbf{x})) \cdots (\mathbf{n}_P^\top \mathbf{m}_P(\mathbf{x})) (\mathbf{y}^\top \mathbf{f}(\mathbf{x})). \quad (11)$$

By the orthogonality property $\nabla N_p(\mathbf{x})^\top \mathbf{m}_q(\mathbf{x}) = \delta_{pq}$, we observe that

$$\tilde{G}(\mathbf{x})[\nabla N_1(\mathbf{x}), \dots, \nabla N_P(\mathbf{x}), \mathbf{y}] := \mathbf{y}^\top \mathbf{f}(\mathbf{x}); \quad (12)$$

furthermore, by the orthogonality $\nabla N_p(\mathbf{x})^\top \mathbf{f}(\mathbf{x}) = 0$ (inherent in the conservation of N_p) this evaluates to zero under any non-trivial permutation of the arguments. Now define $\tilde{F}(\mathbf{x}) := \text{Alt } \tilde{G}(\mathbf{x}) \in \text{Alt}^{P+1} \mathbb{R}^d$ to be the alternatisation of $\tilde{G}(\mathbf{x})$. This $\tilde{F}(\mathbf{x})$ is alternating for all arguments by construction, and coincides with $\tilde{G}(\mathbf{x})$ when evaluated at $[\nabla N_1(\mathbf{x}), \dots, \nabla N_P(\mathbf{x}), \mathbf{y}]$ for any \mathbf{y} , since all but the trivial permutation evaluate to zero in the alternatisation (9). Hence (10) holds. \square

Since the proof here is constructive, one may potentially use it directly when seeking to define such an \tilde{F} . In simpler cases however, such an \tilde{F} can often be found by inspection, as we will demonstrate for the Kepler problem in Section 2.1 below.

With Theorem 2.3 established and \tilde{F} defined, we may now apply the same general strategy described in [3] to construct an integrator for (1) that preserves all conservation laws. We introduce auxiliary variables $(\widetilde{\nabla N}_p) \in \dot{\mathbb{X}}_n^P$, approximating $(\nabla N_p(\mathbf{x}))$, such that

$$\mathcal{I}_n \left[\widetilde{\nabla N}_p^\top \mathbf{y}_p \right] = \int_{T_n} \nabla N_p(\mathbf{x})^\top \mathbf{y}_p, \quad (13)$$

for all $(\mathbf{y}_p)_{p=1}^P \in \dot{\mathbb{X}}_n^P$. The general conservative scheme is then: find $(\mathbf{x}, (\widetilde{\nabla N}_p)) \in \mathbb{X}_n \times \dot{\mathbb{X}}_n^P$ such that

$$\mathcal{I}_n \left[\mathbf{y}^\top \dot{\mathbf{x}} \right] = \mathcal{I}_n \left[\tilde{F}(\mathbf{x})[\widetilde{\nabla N}_1, \dots, \widetilde{\nabla N}_P, \mathbf{y}] \right], \quad (14a)$$

$$\mathcal{I}_n \left[\widetilde{\nabla N}_p^\top \mathbf{y}_p \right] = \int_{T_n} \nabla N_p(\mathbf{x})^\top \mathbf{y}_p, \quad p = 1, \dots, P, \quad (14b)$$

for all $(\mathbf{y}, (\mathbf{y}_p)) \in \dot{\mathbb{X}}_n \times \dot{\mathbb{X}}_n^P$.

Theorem 2.4 (Conservation properties of (14)). *Assuming solutions exist, the integrator (14) satisfies $N_p(\mathbf{x}(t_{n+1})) = N_p(\mathbf{x}(t_n))$ for all p .*

Proof. For each p , by considering respectively $\mathbf{y}_p = \dot{\mathbf{x}}$ in (14b) and $\mathbf{y} = \widetilde{\nabla N}_p$ in (14a),

$$N_p(\mathbf{x}(t_{n+1})) - N_p(\mathbf{x}(t_n)) = \int_{T_n} \dot{N}_p = \int_{T_n} \nabla N_p(\mathbf{x})^\top \dot{\mathbf{x}} = \mathcal{I}_n \left[\widetilde{\nabla N}_p^\top \dot{\mathbf{x}} \right] = \mathcal{I}_n \left[\tilde{F}(\mathbf{x})[\widetilde{\nabla N}_1, \dots, \widetilde{\nabla N}_P, \widetilde{\nabla N}_p] \right] = 0, \quad (15)$$

where the final equality holds by the alternating property of $\tilde{F}(\mathbf{x})$. \square

Remark 2.5. *As with (7), the auxiliary variables introduced in (14) can always be eliminated, and thus incur very little additional computational cost.*

2.1. Kepler problem

As a numerical demonstration of the scheme (14) we discretise the nondimensionalised two-body Kepler problem,

$$\dot{\mathbf{x}} = \mathbf{v}, \quad \dot{\mathbf{v}} = -\frac{1}{\|\mathbf{x}\|^3} \mathbf{x}, \quad (16)$$

for $\mathbf{x}, \mathbf{v} : \mathbb{R}_+ \rightarrow \mathbb{R}^d$ representing the position and velocity respectively, and $\|\cdot\|$ denoting the ℓ^2 norm. Trajectories of (16) preserve the energy H , angular momentum \mathbf{L} , and Runge–Lenz vector \mathbf{A} , defined as

$$H(\mathbf{x}, \mathbf{v}) := \frac{1}{2} \|\mathbf{v}\|^2 - \frac{1}{\|\mathbf{x}\|}, \quad \mathbf{L}(\mathbf{x}, \mathbf{v}) := \mathbf{x} \times \mathbf{v}, \quad \mathbf{A}(\mathbf{x}, \mathbf{v}) := \mathbf{v} \times \mathbf{L}(\mathbf{x}, \mathbf{v}) - \frac{1}{\|\mathbf{x}\|} \mathbf{x}, \quad (17)$$

where \times denotes the cross product. Roughly speaking, H and \mathbf{L} encode the shape of the orbit and the plane to which it is restricted, whereas the orientation of the orbit within that plane is encoded in \mathbf{A} [16]. These invariants are not

independent, as $\|\mathbf{A}\|^2 = 1 + 2H\|\mathbf{L}\|^2$, while \mathbf{A} and \mathbf{L} are necessarily orthogonal; these 3 invariants thus represent $2d - 1$ independent constants of motion (for $d \in \{2, 3\}$), the maximum possible number of conserved quantities.

We consider the two-dimensional case $d = 2$. In this case, if H and $\mathbf{A} = (A_1, A_2)$ are conserved, then the scalar angular momentum $L = \|\mathbf{L}\|$ will be conserved automatically, since $\|\mathbf{A}\|^2 = 1 + 2HL^2$. We may therefore construct a fully conservative numerical integrator for $d = 2$ using our scheme (14) by conserving the $P = 3$ independent invariants H, A_1 , and A_2 .

To apply (14) we must construct some $\tilde{F} : \mathbb{R}^{2 \times 2} \rightarrow \text{Alt}^4 \mathbb{R}^{2 \times 2}$ satisfying the conditions of (10), i.e. such that $\forall (\mathbf{x}, \mathbf{v}), (\mathbf{y}, \mathbf{w}) \in \mathbb{R}^{2 \times 2}$,

$$\mathbf{y}^\top \mathbf{v} - \mathbf{w}^\top \frac{1}{\|\mathbf{x}\|^3} \mathbf{x} = \tilde{F} \left(\begin{pmatrix} \mathbf{x} \\ \mathbf{v} \end{pmatrix} \right) \left[\begin{pmatrix} \nabla_{\mathbf{x}} H \\ \nabla_{\mathbf{v}} H \end{pmatrix}, \begin{pmatrix} \nabla_{\mathbf{x}} A_1 \\ \nabla_{\mathbf{v}} A_1 \end{pmatrix}, \begin{pmatrix} \nabla_{\mathbf{x}} A_2 \\ \nabla_{\mathbf{v}} A_2 \end{pmatrix}, \begin{pmatrix} \mathbf{y} \\ \mathbf{w} \end{pmatrix} \right], \quad (18)$$

where $\nabla_{\mathbf{x}}, \nabla_{\mathbf{v}}$ denote gradients with respect to \mathbf{x}, \mathbf{v} respectively. Instead of using the constructive proof in Theorem 2.3, we may more simply note the space $\text{Alt}^4 \mathbb{R}^4$ only has dimension 1; any alternating n -form in n dimensions is some multiple of the determinant map on the n -by- n square matrix formed by the n argument vectors. This allows us to substantially reduce the space of potential maps \tilde{F} to consider. Noting the gradients of our conserved quantities,

$$\nabla_{\mathbf{x}} H = \frac{1}{\|\mathbf{x}\|^3} \mathbf{x}, \quad \nabla_{\mathbf{x}} \mathbf{A} = \frac{1}{\|\mathbf{x}\|^3} \mathbf{x} \otimes \mathbf{x} - \mathbf{v} \otimes \mathbf{v} + \left(\|\mathbf{v}\|^2 - \frac{1}{\|\mathbf{x}\|} \right) I, \quad (19a)$$

$$\nabla_{\mathbf{v}} H = \mathbf{v}, \quad \nabla_{\mathbf{v}} \mathbf{A} = 2\mathbf{x} \otimes \mathbf{v} - \mathbf{v} \otimes \mathbf{x} - (\mathbf{x} \cdot \mathbf{v}) I, \quad (19b)$$

where \otimes denotes the outer product, we may see by inspection that, for all $(\mathbf{x}, \mathbf{v}), (\mathbf{y}, \mathbf{w}) \in \mathbb{R}^{2 \times 2}$,

$$\frac{1}{2L(\mathbf{x}, \mathbf{v})H(\mathbf{x}, \mathbf{v})} \det \begin{bmatrix} \mathbf{y} & \nabla_{\mathbf{x}} H & \nabla_{\mathbf{x}} \mathbf{A}^\top \\ \mathbf{w} & \nabla_{\mathbf{v}} H & \nabla_{\mathbf{v}} \mathbf{A}^\top \end{bmatrix} = \mathbf{y}^\top \mathbf{v} - \mathbf{w}^\top \frac{1}{\|\mathbf{x}\|^3} \mathbf{x}, \quad (20)$$

where $\det : \mathbb{R}^{4 \times 4} \rightarrow \mathbb{R}$ denotes the determinant map. We may therefore define $\tilde{F} : \mathbb{R}^{2 \times 2} \rightarrow \text{Alt}^4 \mathbb{R}^{2 \times 2}$ as

$$\tilde{F} \left(\begin{pmatrix} \mathbf{x} \\ \mathbf{v} \end{pmatrix} \right) \left[\begin{pmatrix} \widetilde{\nabla_{\mathbf{x}} H} \\ \widetilde{\nabla_{\mathbf{v}} H} \end{pmatrix}, \begin{pmatrix} \widetilde{\nabla_{\mathbf{x}} A_1} \\ \widetilde{\nabla_{\mathbf{v}} A_1} \end{pmatrix}, \begin{pmatrix} \widetilde{\nabla_{\mathbf{x}} A_2} \\ \widetilde{\nabla_{\mathbf{v}} A_2} \end{pmatrix}, \begin{pmatrix} \mathbf{y} \\ \mathbf{w} \end{pmatrix} \right] := \frac{1}{2L(\mathbf{x}, \mathbf{v})H(\mathbf{x}, \mathbf{v})} \det \begin{bmatrix} \mathbf{y} & \widetilde{\nabla_{\mathbf{x}} H} & \widetilde{\nabla_{\mathbf{x}} A_1} & \widetilde{\nabla_{\mathbf{x}} A_2} \\ \mathbf{w} & \widetilde{\nabla_{\mathbf{v}} H} & \widetilde{\nabla_{\mathbf{v}} A_1} & \widetilde{\nabla_{\mathbf{v}} A_2} \end{bmatrix}, \quad (21)$$

which satisfies (10) by (20), and can be seen to be an alternating form by the alternating properties of the determinant.

Through (14) we then arrive at our fully conservative integrator for the two-dimensional Kepler problem: find $((\mathbf{x}, \mathbf{v}), (\nabla_{\mathbf{x}} H, \nabla_{\mathbf{v}} H), (\nabla_{\mathbf{x}} \mathbf{A}, \nabla_{\mathbf{v}} \mathbf{A})) \in \mathbb{X}_n \times \mathbb{X}_n \times \mathbb{X}_n^2$ (with \mathbb{X}_n defined as in (5) for $d = 2 \times 2$) such that

$$\mathcal{I}_n [\mathbf{y}^\top \dot{\mathbf{x}} + \mathbf{w}^\top \dot{\mathbf{v}}] = \mathcal{I}_n \left[\frac{1}{2L(\mathbf{x}, \mathbf{v})H(\mathbf{x}, \mathbf{v})} \det \begin{bmatrix} \mathbf{y} & \widetilde{\nabla_{\mathbf{x}} H} & \widetilde{\nabla_{\mathbf{x}} \mathbf{A}}^\top \\ \mathbf{w} & \widetilde{\nabla_{\mathbf{v}} H} & \widetilde{\nabla_{\mathbf{v}} \mathbf{A}}^\top \end{bmatrix} \right], \quad (22a)$$

$$\mathcal{I}_n [\widetilde{\nabla_{\mathbf{x}} H}^\top \mathbf{y}_H + \widetilde{\nabla_{\mathbf{v}} H}^\top \mathbf{w}_H] = \int_{T_n} \nabla H(\mathbf{x}, \mathbf{v})^\top \mathbf{y}_H + \nabla H(\mathbf{x}, \mathbf{v})^\top \mathbf{w}_H, \quad (22b)$$

$$\mathcal{I}_n [\text{tr}(\widetilde{\nabla_{\mathbf{x}} \mathbf{A}} Y_A + \widetilde{\nabla_{\mathbf{v}} \mathbf{A}} W_A)] = \int_{T_n} \text{tr}(\nabla_{\mathbf{x}} \mathbf{A}(\mathbf{x}, \mathbf{v}) Y_A + \nabla_{\mathbf{v}} \mathbf{A}(\mathbf{x}, \mathbf{v}) W_A), \quad (22c)$$

for all $((\mathbf{y}, \mathbf{w}), (\mathbf{y}_H, \mathbf{w}_H), (Y_A, W_A)) \in \mathbb{X}_n \times \mathbb{X}_n \times \mathbb{X}_n^2$, where tr denotes the trace.

We test the fully conservative integrator (22) numerically on a standard set of ICs (inspired by [12, Sec. I.2.3]) given by $\mathbf{x}(0) = (0.4, 0)$, $\mathbf{v}(0) = (0, 2)$. In each of these tests, we take \mathcal{I}_n to be an s -stage Gauß–Legendre quadrature, such that the scheme (22) is a conservative modification of a Gauß method of the same order.

2.1.1. Comparison test

To illustrate the qualitative benefits afforded by the fully conservative scheme (22), Figure 1 solves the Kepler problem with timestep $\Delta t_n = 0.1$ and final time $t = 100$, using various classical 1-stage, 2nd-order implicit geometric integrators: implicit midpoint (IM), the mean-value (or averaged-vector-field) discrete-gradient (MV–DG) method of McLachlan, Quispel & Robidoux [14], the LaBudde–Greenspan (LB–G) energy- and angular momentum-conservative scheme [17], and our scheme (22) at $s = 1$.

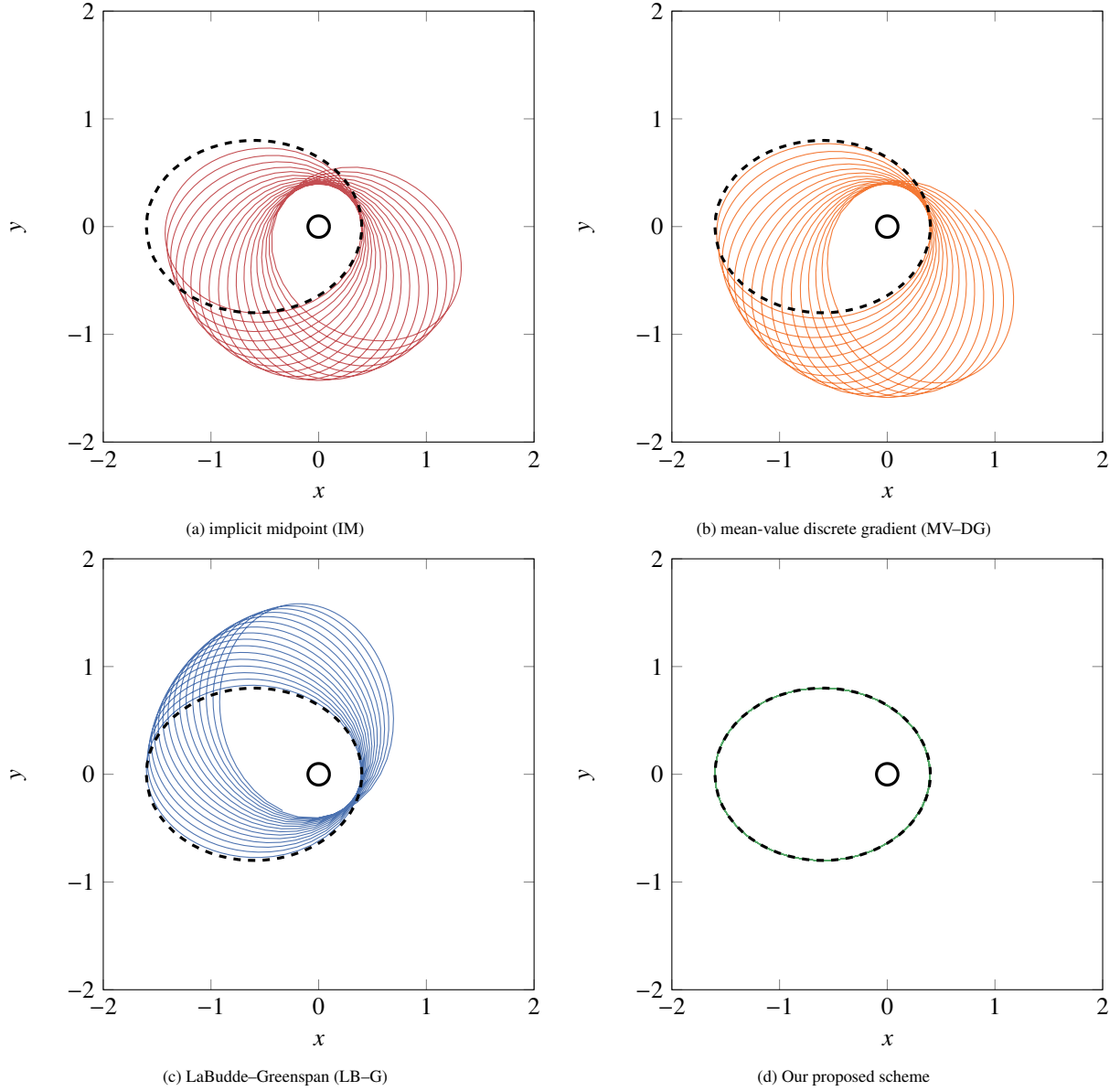


Figure 1: Trajectories of the Kepler problem. The exact solution is given by the dashed ellipse. All schemes are of the same order.

In those cases where they are not conserved, Figure 2 shows the evolution of the invariants H , L , θ up to time $t = 50$, where $\theta := \arg \mathbf{A}$.

As a symplectic method, implicit midpoint conserves the quadratic invariant L (up to quadrature error, solver tolerances and machine precision) but neither H nor θ ; it therefore conserves neither the orbit shape nor its orientation, since trajectories in the Kepler problem should be precession-free. The mean-value discrete gradient scheme conserves H , but neither L nor θ . The scheme of LaBudde & Greenspan conserves H and L by design, and so conserves the orbit shape, but not its orientation θ . In contrast, our scheme (22) conserves all three invariants, thereby restricting the discrete solution to the same ellipse traced out by the exact solution.

These results illustrate the potential importance of conserving invariants in Poisson (and non-Poisson) systems: while symplectic methods are likely preferable for e.g. capturing the statistical behaviour of chaotic systems, conservative discretisations may give more physically reasonable results for individual trajectories at coarser timesteps.

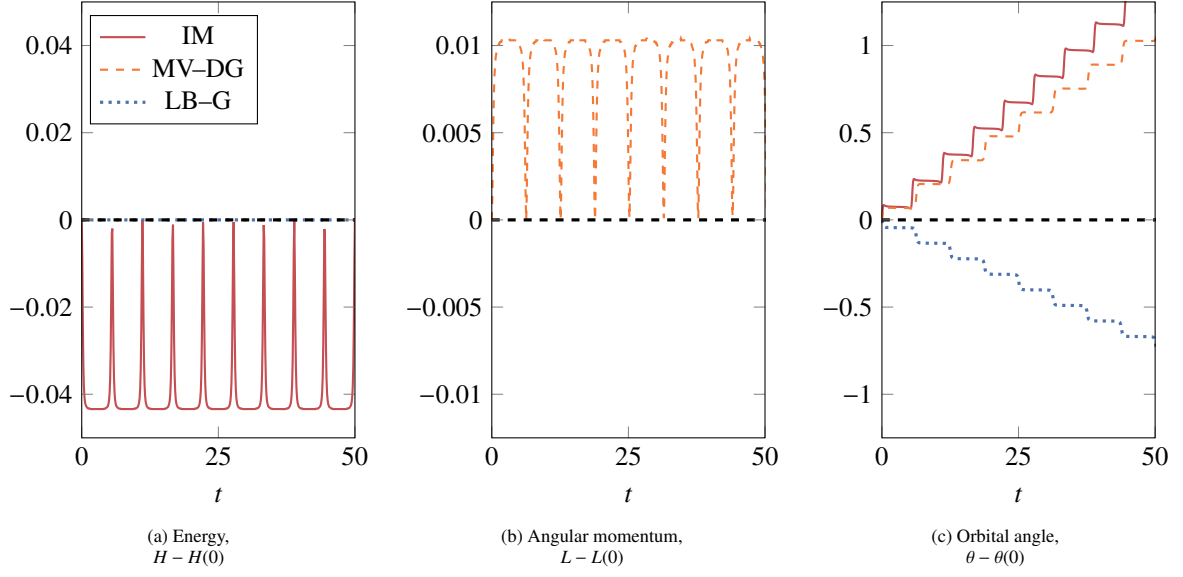


Figure 2: Error in scalar invariants of the Kepler problem: H , L and θ .

2.1.2. Convergence test

Figure 3 shows the convergence of (22), as measured by the error in the position of the orbital body after the true orbital period (2π for these ICs) at varying timesteps Δt_n and stages s . As with the underlying Gauß scheme, we observe convergence with rate $2s$ before round-off errors dominate.

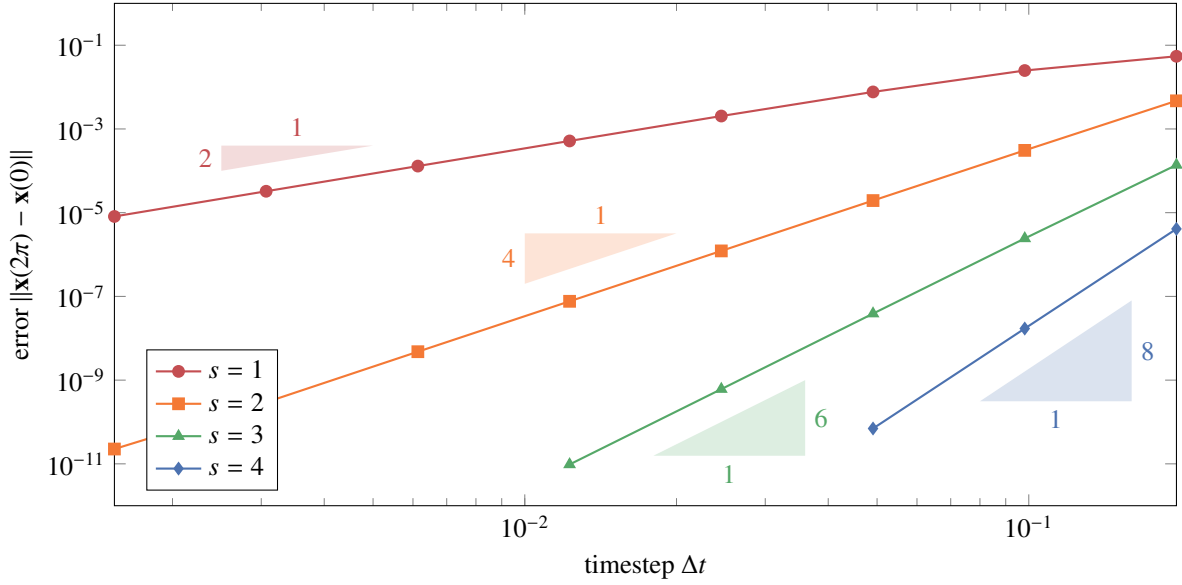


Figure 3: Error in the position of the orbital body at $t = 2\pi$ for varying timesteps $\Delta t \in 2\pi \cdot 2^k$, $k \in \{-5, \dots, -12\}$ and stages $s \in \{1, \dots, 4\}$. The convergence curve for $s \in \{3, 4\}$ flattens out at smaller timesteps due to round-off error and solver tolerances. Triangles demonstrate observed convergence rates of $2s$.

2.2. Kovalevskaya problem

As a further example, we consider the nondimensionalised Kovalevskaya top [18],

$$\dot{\mathbf{n}} = \mathbf{n} \times J\mathbf{l}, \quad \dot{\mathbf{l}} = \mathbf{n} \times \mathbf{e}_1 + \mathbf{l} \times J\mathbf{l}, \quad (23)$$

for $\mathbf{n}, \mathbf{l} : \mathbb{R}_+ \rightarrow \mathbb{R}^3$ representing the orientation vector (i.e. the z -components of the principal axes) and the angular momentum (i.e. the components of the angular momentum along those principal axes) respectively, \mathbf{e}_1 denoting the basis vector $(1, 0, 0)$, and J denoting the matrix

$$J := \begin{pmatrix} 1 & 0 & 0 \\ 0 & 1 & 0 \\ 0 & 0 & 2 \end{pmatrix}. \quad (24)$$

Trajectories of this system have 4 invariants: the energy $H := \frac{1}{2}\mathbf{l}^\top J\mathbf{l}$, the (square) norm of the orientation vector $\|\mathbf{n}\|^2$, the angular momentum in the z direction $L = \mathbf{l} \cdot \mathbf{n}$, and the Kovalevskaya invariant $K = |\xi|^2$ where $\xi = (l_1 + il_2)^2 - 2(n_1 + in_2)$ (i is the imaginary unit). While $H, \|\mathbf{n}\|^2$ and $\mathbf{l} \cdot \mathbf{n}$ are quadratic, K is quartic.

Unlike the Kepler problem discussed above, it is not immediately clear from inspection how one might define an $\tilde{F} : \mathbb{R}^6 \rightarrow \text{Alt}^5 \mathbb{R}^6$ satisfying the conditions of Theorem 2.3; we therefore find such an \tilde{F} using a construction similar to that used in the proof of Theorem 2.3. Define the multilinear map $\tilde{G}((\mathbf{n}, \mathbf{l})) : (\mathbb{R}^6)^5 \rightarrow \mathbb{R}$,

$$\tilde{G}\left(\begin{pmatrix} \mathbf{n} \\ \mathbf{l} \end{pmatrix}\right)\left[\begin{pmatrix} \mathbf{a}_1 \\ \mathbf{b}_1 \end{pmatrix}, \begin{pmatrix} \mathbf{a}_2 \\ \mathbf{b}_2 \end{pmatrix}, \begin{pmatrix} \mathbf{a}_3 \\ \mathbf{b}_3 \end{pmatrix}, \begin{pmatrix} \mathbf{a}_4 \\ \mathbf{b}_4 \end{pmatrix}, \begin{pmatrix} \mathbf{m} \\ \mathbf{k} \end{pmatrix}\right] := \det[\mathbf{b}_1 \ \mathbf{b}_2 \ \mathbf{b}_3] (\mathbf{n} \cdot \mathbf{a}_4) \left[\mathbf{m}^\top (\mathbf{n} \times J\mathbf{l}) + \mathbf{k}^\top (\mathbf{n} \times \mathbf{e}_1) + \mathbf{k}^\top (\mathbf{l} \times J\mathbf{l}) \right]. \quad (25a)$$

Considering the alternatisation $\text{Alt } \tilde{G}((\mathbf{n}, \mathbf{l})) \in \text{Alt}^5 \mathbb{R}^6$, if we apply $\text{Alt } \tilde{G}((\mathbf{n}, \mathbf{l}))$ to the gradients of the invariants $H, K, L, \frac{1}{2}\|\mathbf{n}\|^2$ respectively, we see

$$\text{Alt } \tilde{G}\left(\begin{pmatrix} \mathbf{n} \\ \mathbf{l} \end{pmatrix}\right)\left[\begin{pmatrix} \mathbf{e}_1 \\ J\mathbf{l} \end{pmatrix}, \begin{pmatrix} \nabla_{\mathbf{n}} K \\ \nabla_{\mathbf{l}} K \end{pmatrix}, \begin{pmatrix} \mathbf{l} \\ \mathbf{n} \end{pmatrix}, \begin{pmatrix} \mathbf{n} \\ \mathbf{0} \end{pmatrix}, \begin{pmatrix} \mathbf{m} \\ \mathbf{k} \end{pmatrix}\right] = 6 \det[J\mathbf{l} \ \nabla_{\mathbf{l}} K \ \mathbf{n}] \|\mathbf{n}\|^2 \left[\mathbf{m}^\top (\mathbf{n} \times J\mathbf{l}) + \mathbf{k}^\top (\mathbf{n} \times \mathbf{e}_1) + \mathbf{k}^\top (\mathbf{l} \times J\mathbf{l}) \right]. \quad (25b)$$

We therefore define $\tilde{F}((\mathbf{n}, \mathbf{l})) \in \text{Alt}^5 \mathbb{R}^6$,

$$\tilde{F}\left(\begin{pmatrix} \mathbf{n} \\ \mathbf{l} \end{pmatrix}\right)\left[\begin{pmatrix} \mathbf{a}_1 \\ \mathbf{b}_1 \end{pmatrix}, \begin{pmatrix} \mathbf{a}_2 \\ \mathbf{b}_2 \end{pmatrix}, \begin{pmatrix} \mathbf{a}_3 \\ \mathbf{b}_3 \end{pmatrix}, \begin{pmatrix} \mathbf{a}_4 \\ \mathbf{b}_4 \end{pmatrix}, \begin{pmatrix} \mathbf{m} \\ \mathbf{k} \end{pmatrix}\right] := \frac{1}{6 \det[J\mathbf{l} \ \nabla_{\mathbf{l}} K \ \mathbf{n}] \|\mathbf{n}\|^2} \text{Alt } \tilde{G}\left(\begin{pmatrix} \mathbf{n} \\ \mathbf{l} \end{pmatrix}\right)\left[\begin{pmatrix} \mathbf{a}_1 \\ \mathbf{b}_1 \end{pmatrix}, \begin{pmatrix} \mathbf{a}_2 \\ \mathbf{b}_2 \end{pmatrix}, \begin{pmatrix} \mathbf{a}_3 \\ \mathbf{b}_3 \end{pmatrix}, \begin{pmatrix} \mathbf{a}_4 \\ \mathbf{b}_4 \end{pmatrix}, \begin{pmatrix} \mathbf{m} \\ \mathbf{k} \end{pmatrix}\right]. \quad (25c)$$

This satisfies (10). We may then use this \tilde{F} in (14) to define a fully conservative integrator for the Kovalevskaya top.

2.2.1. Numerical test

Figure 4 shows numerical simulations of the Kovalevskaya top with both implicit midpoint, and the fully conservative modification of 1-stage continuous Petrov–Galerkin (14) (i.e. setting \mathcal{I}_n to be the exact integral) using \tilde{F} as in (25c). We use the same ICs $\mathbf{n}(0) = (0.8, 0.6, 0)$, $\mathbf{l}(0) = (2, 0, 0.2)$ in either case, and a uniform timestep $\Delta t_n = 0.1$, up to a final time $t = 300$. Figure 5 shows the evolution and drift of the Kovalevskaya invariant K within the implicit midpoint scheme. In both figures, colouring indicates error in the Kovalevskaya invariant K : green for $|K - K(0)| \leq \frac{1}{2}$, orange for $|K - K(0)| \in (\frac{1}{2}, 1]$, red for $|K - K(0)| > 1$.

All invariants, including K , are conserved by the trajectory of our scheme (up to quadrature error, solver tolerances and machine precision). As a quartic invariant, K is not conserved by implicit midpoint; we see that the resulting drift in K allows the numerical simulation to admit unphysical trajectories after a sufficient duration (approximately 18 rotations of the top for these ICs).

3. GENERIC ODEs

We now turn to systems of ODEs in the GENERIC formalism [4, 5], which couple reversible (Poisson) and irreversible (gradient-descent) dynamics in a thermodynamically compatible way. The general GENERIC ODE has the form

$$\dot{\mathbf{x}} = B(\mathbf{x})\nabla E(\mathbf{x}) + D(\mathbf{x})\nabla S(\mathbf{x}), \quad (26)$$

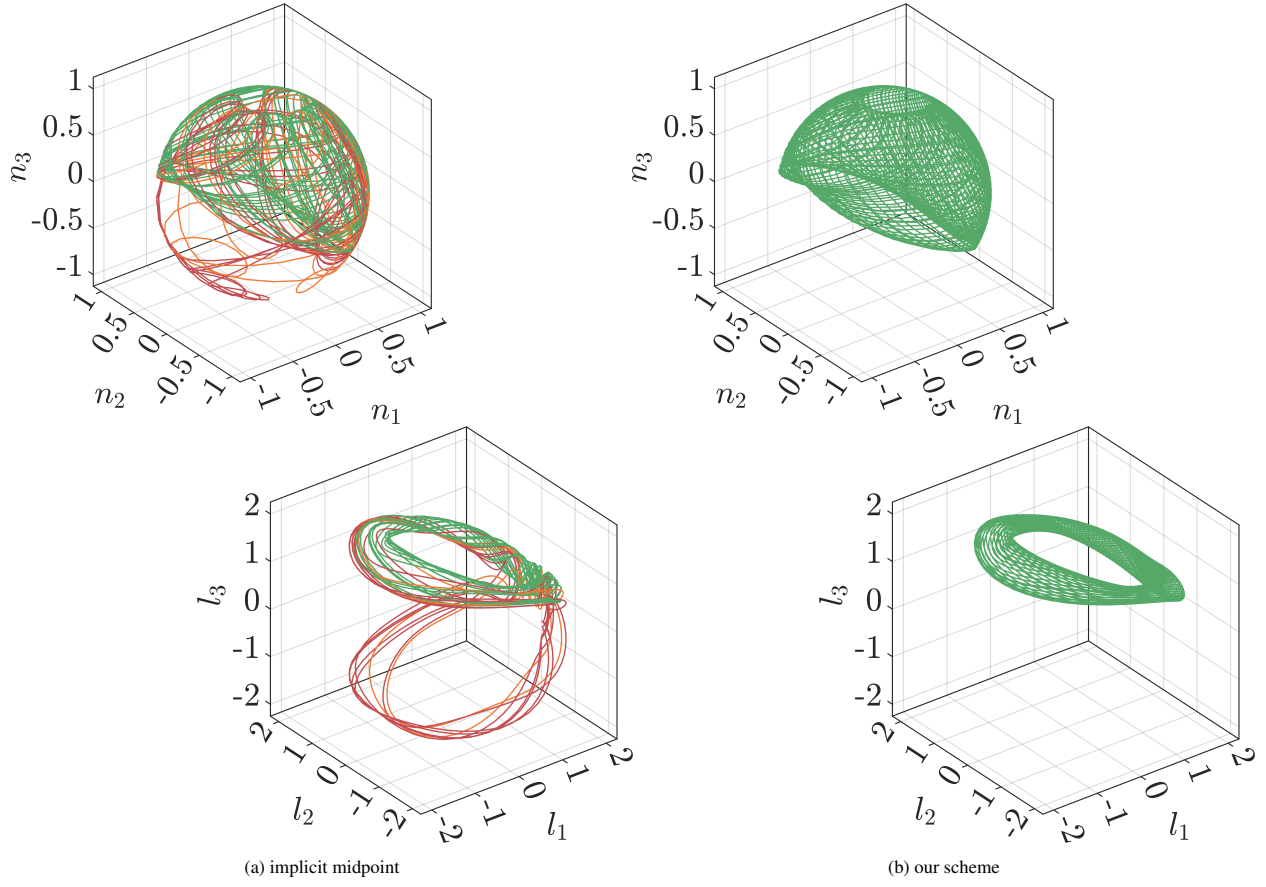


Figure 4: Trajectories in \mathbf{n}, \mathbf{l} of the Kovalevskaya top, with implicit midpoint (left) and our proposed scheme (right).

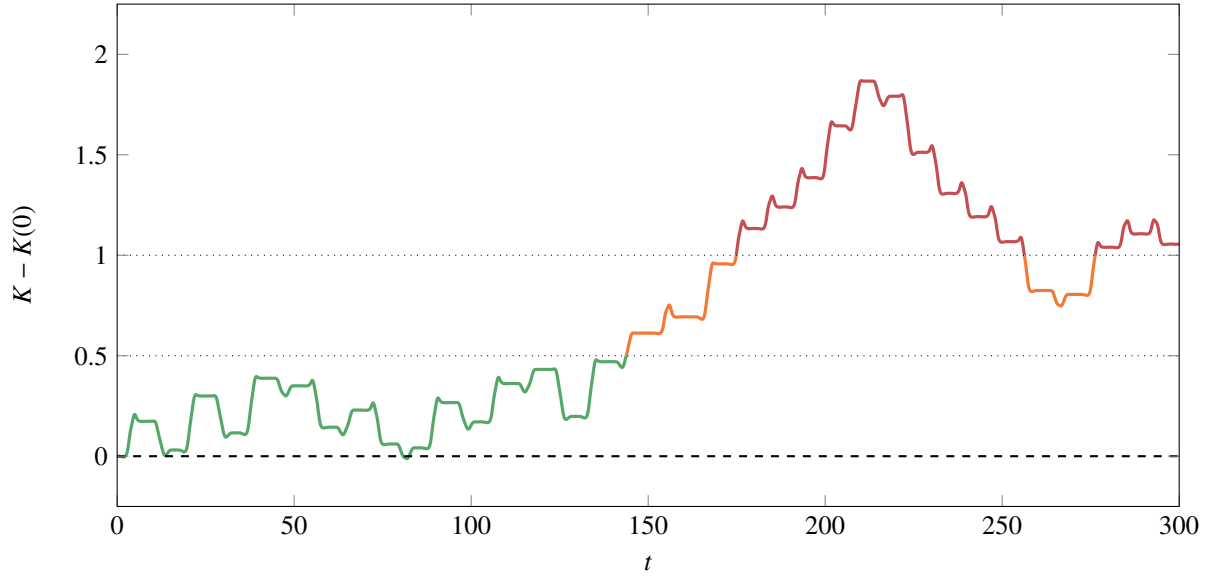


Figure 5: Error $K - K(0)$ within the implicit midpoint simulation of the Kovalevskaya top.

where $B(\mathbf{x}), D(\mathbf{x}) \in \mathbb{R}^{d \times d}$ are respectively skew-symmetric and positive-semidefinite (the Poisson and friction matrices), and $E, S : \mathbb{R}^d \rightarrow \mathbb{R}$ denote the energy and entropy. This augments the general Poisson system (3) with an additional dissipative contribution. Thermodynamic consistency imposes the orthogonality (degeneracy) conditions

$$\nabla S(\mathbf{x})^\top B(\mathbf{x}) = \mathbf{0}^\top, \quad \nabla E(\mathbf{x})^\top D(\mathbf{x}) = \mathbf{0}^\top. \quad (27)$$

We see these conditions ensure energy conservation ($\frac{d}{dt}E(\mathbf{x}) = 0$) and entropy generation ($\frac{d}{dt}S(\mathbf{x}) \geq 0$) along exact trajectories by testing (26) against ∇E and ∇S . To preserve these thermodynamic properties on the discrete level, the strategy in the construction of (7) and (14) then suggests (i) introducing auxiliary variables $\widetilde{\nabla E}$ and $\widetilde{\nabla S}$ approximating ∇E and ∇S respectively, and (ii) introducing these in the right-hand side of (26). It is, however, insufficient to substitute these auxiliary variables only for the gradients seen in (26), as this will fail to reproduce the orthogonality conditions (27). We therefore assume access to certain consistent extensions of B and D that can be evaluated on these auxiliary variables.

Assumption 3.1 (Characterisation of GENERIC matrix compatibility). *Assume the existence of $\tilde{B}, \tilde{D} : (\mathbb{R}^d)^2 \rightarrow \mathbb{R}^{d \times d}$ such that the following hold:*

1. *Consistency with B, D : for all $\mathbf{x} \in \mathbb{R}^d$,*

$$\tilde{B}(\mathbf{x}, \nabla S(\mathbf{x})) = B(\mathbf{x}), \quad \tilde{D}(\mathbf{x}, \nabla E(\mathbf{x})) = D(\mathbf{x}). \quad (28a)$$

2. *Skew-symmetry and positive-semidefiniteness: for all $\mathbf{x}, \widetilde{\nabla E}, \widetilde{\nabla S} \in \mathbb{R}^d$, $\tilde{B}(\mathbf{x}, \widetilde{\nabla S})$ is skew-symmetric, and $\tilde{D}(\mathbf{x}, \widetilde{\nabla E})$ is positive-semidefinite.*

3. *Preservation of compatibility (27): for all $\mathbf{x}, \widetilde{\nabla E}, \widetilde{\nabla S} \in \mathbb{R}^d$,*

$$\widetilde{\nabla S}^\top \tilde{B}(\mathbf{x}, \widetilde{\nabla S}) = \mathbf{0}^\top, \quad \widetilde{\nabla E}^\top \tilde{D}(\mathbf{x}, \widetilde{\nabla E}) = \mathbf{0}^\top. \quad (28b)$$

Remark 3.2. While we cannot guarantee Theorem 3.1 always holds in full generality, it holds in the typical cases we consider below, and suffices for our discrete stability results.

With this in hand, the GENERIC ODE (26) can be discretised in an energy- and entropy-stable manner by defining auxiliary variables $\widetilde{\nabla E}, \widetilde{\nabla S} \in \mathbb{X}_n$, introducing these into the right-hand side, and substituting the Poisson and friction matrices for their consistent extensions evaluated at these auxiliary variables: find $(\mathbf{x}, (\widetilde{\nabla E}, \widetilde{\nabla S})) \in \mathbb{X}_n \times (\mathbb{X}_n)^2$ such that, for all $(\mathbf{y}, (\mathbf{y}_E, \mathbf{y}_S)) \in \mathbb{X}_n \times (\mathbb{X}_n)^2$,

$$\mathcal{I}_n[\mathbf{y}^\top \dot{\mathbf{x}}] = \mathcal{I}_n[\mathbf{y}^\top \tilde{B}(\mathbf{x}, \widetilde{\nabla S}) \widetilde{\nabla E} + \mathbf{y}^\top \tilde{D}(\mathbf{x}, \widetilde{\nabla E}) \widetilde{\nabla S}], \quad (29a)$$

$$\mathcal{I}_n[\widetilde{\nabla E}^\top \mathbf{y}_E] = \int_{T_n} \nabla E(\mathbf{x})^\top \mathbf{y}_E, \quad (29b)$$

$$\mathcal{I}_n[\widetilde{\nabla S}^\top \mathbf{y}_S] = \int_{T_n} \nabla S(\mathbf{x})^\top \mathbf{y}_S. \quad (29c)$$

Theorem 3.3 (Energy and entropy stability of (29)). *Assuming solutions exist, the integrator (29) is energy- and entropy-stable, with $E(\mathbf{x}(t_{n+1})) = E(\mathbf{x}(t_n))$ and $S(\mathbf{x}(t_{n+1})) \geq S(\mathbf{x}(t_n))$.*

Proof. By considering respectively $\mathbf{y}_E = \dot{\mathbf{x}}$, $\mathbf{y}_S = \dot{\mathbf{x}}$ and $\mathbf{y} = \widetilde{\nabla E}$, $\mathbf{y} = \widetilde{\nabla S}$ in (29),

$$\begin{aligned} E(\mathbf{x}(t_{n+1})) - E(\mathbf{x}(t_n)) &= \int_{T_n} \dot{E} \\ &= \int_{T_n} \nabla E(\mathbf{x})^\top \dot{\mathbf{x}} \\ &= \mathcal{I}_n[\widetilde{\nabla E}^\top \dot{\mathbf{x}}] \end{aligned} \quad \begin{aligned} S(\mathbf{x}(t_{n+1})) - S(\mathbf{x}(t_n)) &= \int_{T_n} \dot{S} \\ &= \int_{T_n} \nabla S(\mathbf{x})^\top \dot{\mathbf{x}} \\ &= \mathcal{I}_n[\widetilde{\nabla S}^\top \dot{\mathbf{x}}] \end{aligned} \quad (30a)$$

$$\begin{aligned} &= \mathcal{I}_n \left[\widetilde{\nabla E}^\top \tilde{B}(\mathbf{x}, \widetilde{\nabla S}) \widetilde{\nabla E} + \widetilde{\nabla E}^\top \tilde{D}(\mathbf{x}, \widetilde{\nabla E}) \widetilde{\nabla S} \right] \\ &= 0, \end{aligned} \quad \begin{aligned} &= \mathcal{I}_n \left[\widetilde{\nabla S}^\top \tilde{B}(\mathbf{x}, \widetilde{\nabla S}) \widetilde{\nabla E} + \widetilde{\nabla S}^\top \tilde{D}(\mathbf{x}, \widetilde{\nabla E}) \widetilde{\nabla S} \right] \\ &\geq 0, \end{aligned} \quad (30b)$$

$$\begin{aligned} &= \mathcal{I}_n \left[\widetilde{\nabla E}^\top \tilde{B}(\mathbf{x}, \widetilde{\nabla S}) \widetilde{\nabla E} + \widetilde{\nabla E}^\top \tilde{D}(\mathbf{x}, \widetilde{\nabla E}) \widetilde{\nabla S} \right] \\ &= 0, \end{aligned} \quad \begin{aligned} &= \mathcal{I}_n \left[\widetilde{\nabla S}^\top \tilde{B}(\mathbf{x}, \widetilde{\nabla S}) \widetilde{\nabla E} + \widetilde{\nabla S}^\top \tilde{D}(\mathbf{x}, \widetilde{\nabla E}) \widetilde{\nabla S} \right] \\ &\geq 0, \end{aligned} \quad (30c)$$

$$\begin{aligned} &= \mathcal{I}_n \left[\widetilde{\nabla E}^\top \tilde{B}(\mathbf{x}, \widetilde{\nabla S}) \widetilde{\nabla E} + \widetilde{\nabla E}^\top \tilde{D}(\mathbf{x}, \widetilde{\nabla E}) \widetilde{\nabla S} \right] \\ &= 0, \end{aligned} \quad \begin{aligned} &= \mathcal{I}_n \left[\widetilde{\nabla S}^\top \tilde{B}(\mathbf{x}, \widetilde{\nabla S}) \widetilde{\nabla E} + \widetilde{\nabla S}^\top \tilde{D}(\mathbf{x}, \widetilde{\nabla E}) \widetilde{\nabla S} \right] \\ &\geq 0, \end{aligned} \quad (30d)$$

$$\begin{aligned} &= 0, \\ &\geq 0, \end{aligned} \quad (30e)$$

where the final equality and inequality hold by Theorem 3.1. \square

Remark 3.4. *Again, as with (7), the auxiliary variables introduced in (29) can be eliminated, incurring little additional computational cost.*

3.1. Internal combustion engine

Inspired by the classical thermodynamic systems considered by e.g. Öttinger [19, Ex. 3] or Gay-Balmaz & Yoshimura [20, Sec. 3.1], we illustrate the GENERIC ODE discretisation (29) with a simple nondimensionalised model of an C -cylinder internal combustion engine, exchanging heat with an isothermal environment. The engine in our model is unfired, i.e. no combustion events are occurring, and coasting, i.e. is spinning on its own inertia alone; together with the environmental heat exchange, this ensures the system is dissipative, fitting into the GENERIC formalism.

Let θ denote the engine phase, measured through an angular displacement, and ω its rate of change. For cylinders $c = 1, \dots, C$ we denote by P_c , T_c , U_c and S_c the pressure, temperature, energy and entropy of the working fluid in cylinder c ; these satisfy constitutive relations associated with the medium, completed by the volume V_c given as a function of θ as

$$V_c := V_p - \cos\left(\theta - \frac{2\pi c}{C}\right), \quad (31)$$

where $V_p > 1$ is an average volume across each piston. We denote the temperature, energy and entropy of the surrounding environment by T_0 , U_0 and S_0 , again coupled by constitutive relations, with T_0 assumed constant. The engine model is then given by

$$\dot{\theta} = \omega, \quad \dot{S}_c = \frac{T_0 - T_c}{T_c}, \quad (32a)$$

$$\dot{\omega} = \sum_{c=1}^C P_c \sin\left(\theta - \frac{2\pi c}{C}\right), \quad \dot{S}_0 = \sum_{c=1}^C \frac{T_c - T_0}{T_0}. \quad (32b)$$

We collect the state as $\mathbf{x} := (\theta, \omega, (S_c)_{c=1}^C, S_0)$, and define the total energy and entropy

$$E(\mathbf{x}) := \frac{1}{2}\omega^2 + \sum_{c=1}^C U_c + U_0, \quad S(\mathbf{x}) := \sum_{c=1}^C S_c + S_0; \quad (33)$$

as above, the energies (U_c) and U_0 may be written as functions of the state \mathbf{x} through the constitutive relations of the medium, with the piston volumes (V_c) given by (31). From the fundamental thermodynamic relations $dU_c = T_c dS_c - P_c dV_c$ and $dU_0 = T_0 dS_0$, we obtain

$$\nabla E(\mathbf{x}) = \begin{pmatrix} -\sum_{c=1}^C P_c \sin\left(\theta - \frac{2\pi c}{C}\right) \\ \omega \\ (T_c)_{c=1}^C \\ T_0 \end{pmatrix}, \quad \nabla S(\mathbf{x}) = \begin{pmatrix} 0 \\ 0 \\ \mathbf{1} \\ 1 \end{pmatrix}. \quad (34)$$

The GENERIC representation (26) of the combustion engine model (32) follows with a Poisson matrix B equal to the canonical 2×2 skew block on (θ, ω) and zeros elsewhere, and a positive-semidefinite friction matrix D encoding thermal relaxation between each cylinder and the environment:

$$B(\mathbf{x}) = \begin{pmatrix} 0 & 1 & 0 & \cdots & 0 & 0 \\ -1 & 0 & 0 & \cdots & 0 & 0 \\ 0 & 0 & 0 & \cdots & 0 & 0 \\ \vdots & \vdots & \vdots & \ddots & \vdots & \vdots \\ 0 & 0 & 0 & \cdots & 0 & 0 \\ 0 & 0 & 0 & \cdots & 0 & 0 \end{pmatrix}, \quad D(\mathbf{x}) = \begin{pmatrix} 0 & 0 & 0 & \cdots & 0 & 0 \\ 0 & 0 & 0 & \cdots & 0 & 0 \\ 0 & 0 & \frac{T_0}{T_1} & & 0 & -1 \\ \vdots & \vdots & & \ddots & \vdots & \\ 0 & 0 & 0 & & \frac{T_0}{T_C} & -1 \\ 0 & 0 & -1 & \cdots & -1 & \sum_{c=1}^C \frac{T_c}{T_0} \end{pmatrix}. \quad (35)$$

The degeneracy conditions (27) hold: $\nabla S(\mathbf{x})^\top B(\mathbf{x}) = \mathbf{0}^\top$ by sparsity, and $\nabla E(\mathbf{x})^\top D(\mathbf{x}) = \mathbf{0}^\top$ by the structure of the thermal block.

For the discrete scheme (29) we require \tilde{B} and \tilde{D} satisfying Theorem 3.1. For the former, we may simply take $\tilde{B} = B$ as B is independent of the state \mathbf{x} ; for the latter, a consistent \tilde{D} may be defined by replacing each temperature T_c with the corresponding components of $\widehat{\nabla E}$:

$$\tilde{D}(\mathbf{x}, \widehat{\nabla E}) := \begin{pmatrix} 0 & 0 & 0 & \cdots & 0 & 0 \\ 0 & 0 & 0 & \cdots & 0 & 0 \\ 0 & 0 & \frac{T_0}{\partial_{S_1} E} & & 0 & -1 \\ \vdots & \vdots & & \ddots & & \vdots \\ 0 & 0 & 0 & & \frac{T_0}{\partial_{S_C} E} & -1 \\ 0 & 0 & -1 & \cdots & -1 & \sum_{c=1}^C \frac{\partial_{S_c} E}{T_0} \end{pmatrix}. \quad (36)$$

Neglecting auxiliary variables that turn out to be constant, the energy- and entropy-stable discretisation given by (29) is then as follows: find $((\theta, \omega, (S_c), S_0), (\tilde{P}, \tilde{\omega}, (\tilde{T}_c)_{c=1}^C)) \in \mathbb{X}_n^{C+3} \times \mathbb{X}_n^{C+2}$ such that, for all $((\eta, \psi, (R_c)_{c=1}^C, R_0), (\tilde{\psi}, \tilde{\eta}, (\tilde{W}_c)_{c=1}^C)) \in \mathbb{X}_n^{C+3} \times \mathbb{X}_n^{C+2}$,

$$\mathcal{I}_n[\dot{\theta}\eta] = \mathcal{I}_n[\tilde{\omega}\eta], \quad (37a)$$

$$\mathcal{I}_n[\dot{\omega}\psi] = -\mathcal{I}_n[\tilde{P}\psi], \quad (37b)$$

$$\mathcal{I}_n[\dot{S}_c R_c] = \mathcal{I}_n\left[\frac{T_0 - \tilde{T}_c}{\tilde{T}_c} R_c\right], \quad c = 1, \dots, C, \quad (37c)$$

$$\mathcal{I}_n[\dot{S}_0 R_0] = \mathcal{I}_n\left[\sum_{c=1}^C \frac{\tilde{T}_c - T_0}{T_0} R_0\right], \quad (37d)$$

$$\mathcal{I}_n[\tilde{P}\tilde{\psi}] = \int_{T_n} \sum_{c=1}^C P_c \sin\left(\theta - \frac{2\pi c}{C}\right) \tilde{\psi}, \quad (37e)$$

$$\mathcal{I}_n[\tilde{\omega}\tilde{\eta}] = \int_{T_n} \omega \tilde{\eta}, \quad (37f)$$

$$\mathcal{I}_n[\tilde{T}_c \tilde{W}_c] = \int_{T_n} T_c \tilde{W}_c, \quad c = 1, \dots, C, \quad (37g)$$

where, for each c , P_c and T_c are functions of S_c and $V_c = V_p - \cos(\theta - 2\pi c/C)$ (31) given by the working fluid's constitutive relations. By Theorem 3.3, the scheme (37) conserves E and is increasing in S (up to machine precision, quadrature and solver tolerances). We observe in fact that the auxiliary variable $\tilde{\omega}$ may be eliminated from the discretisation, by reducing (37a) and (37f) to

$$\mathcal{I}_n[\dot{\theta}\eta] = \int_{T_n} \omega \eta; \quad (38a)$$

similarly, \tilde{P} may be eliminated by reducing (37b) and (37e) to

$$\mathcal{I}_n[\dot{\omega}\psi] = \int_{T_n} \sum_{c=1}^C P_c \sin\left(\theta - \frac{2\pi c}{C}\right) \psi. \quad (38b)$$

3.1.1. Numerical test

To demonstrate the discretisation, we close the system (32) and its discretisation (37) with a fixed equation of state, that of an ideal fluid with heat capacity C_V and adiabatic index $\gamma = 1 + 1/C_V$:

$$P_c = \exp\left(\frac{S_c}{C_V}\right) V_c^{-\gamma}, \quad T_c = P_c V_c, \quad U_c = C_V T_c, \quad U_0 = T_0 S_0. \quad (39)$$

For our experiments, we consider $C_V = 5/2$. We further take $C = 6$ cylinders with average piston volume $V_p = 1 + 2^{-4}$, and assume the system is initially in thermal equilibrium with $T_c(0) = T_0 = 1$ for each c . The initial angular displacement and external entropy are both set to 0, while the initial rate of change of the engine phase is chosen as $\omega(0) = 8$.

Figures 6 & 7 compare the evolution of θ , E and S in numerical simulations of this model engine (32) with both our proposed energy- and entropy-stable integrator (37) taking I_n to be an s -stage Gauß–Legendre method, and the comparable (symplectic) Gauß method. Each simulation is run up to a final time $t = 2^6$, shown alongside a finely-resolved “exact” trajectory computed using our integrator with stages $s = 4$ with a small timestep $\Delta t_n = 2^{-5}$.

Figure 6 uses a timestep $\Delta t_n = 2^{-4}$, with stages $s \in \{1, 2, 3\}$. We see from Figure 6a that our method (37) at lowest order $s = 1$ has a smaller final error in the angular displacement θ than both the 1- and 2-stage Gauß methods; at order $s = 3$, there is no visible difference between the results from our scheme and the “exact” trajectory. From Figure 6c, we see that that our lowest-order ($s = 1$) simulation more accurately reproduces the evolution of the entropy S than the highest-order ($s = 3$) simulation using the Gauß method. Despite the symplectic nature of the Gauß methods, each of the numerical trajectories exhibits a notable final error in the energy E , approximately 3.7, 1.0 and 0.3 for stages $s = 1, 2$ and 3 respectively (compare with the initial value of $E(0) \approx 67.8$).

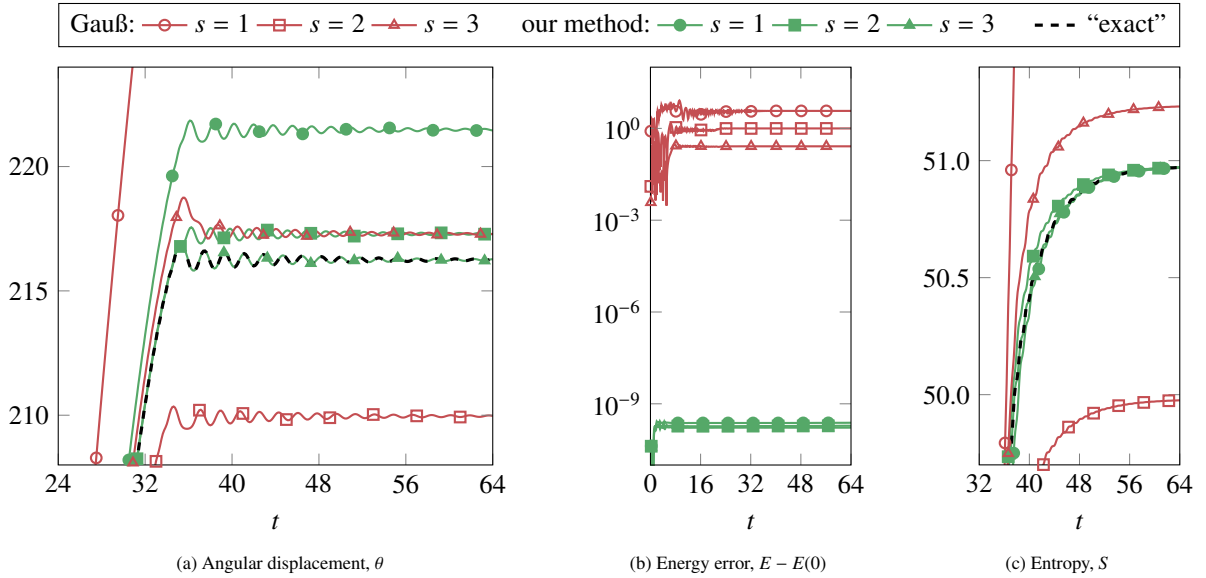


Figure 6: Evolution in θ , E , S for the combustion engine at $\Delta t_n = 2^{-4}$.

Figure 7 uses a longer timestep $\Delta t_n = 2^{-3}$; we consider only the lowest order ($s = 1$) as both the Gauß method and our integrator (37) fail with stages $s > 1^2$. Unlike the numerical results from our method, the angular displacement θ , energy E and entropy S in the implicit midpoint simulation all climb steadily throughout the duration, as the symplectic scheme fails to capture the dissipative effects of the heat exchange. The angle θ reaches a final value of approximately 537 by the end of the simulation; the energy E reaches approximately 125.4 (compare again with $E(0) \approx 67.8$), while the entropy S reaches a final value of approximately 73.8 (compare with the initial value $S(0) \approx 2.3$ and “exact” final value of approximately 51.0).

4. GENERIC PDEs

Having developed the structure-preserving discretisations of finite-dimensional GENERIC systems, we now extend the same thermodynamically consistent framework to the infinite-dimensional setting, with the key ideas carrying

²This represents no real cause for concern, as we have no reason to expect a numerical solution to exist for such implicit multistage methods at such long timesteps.

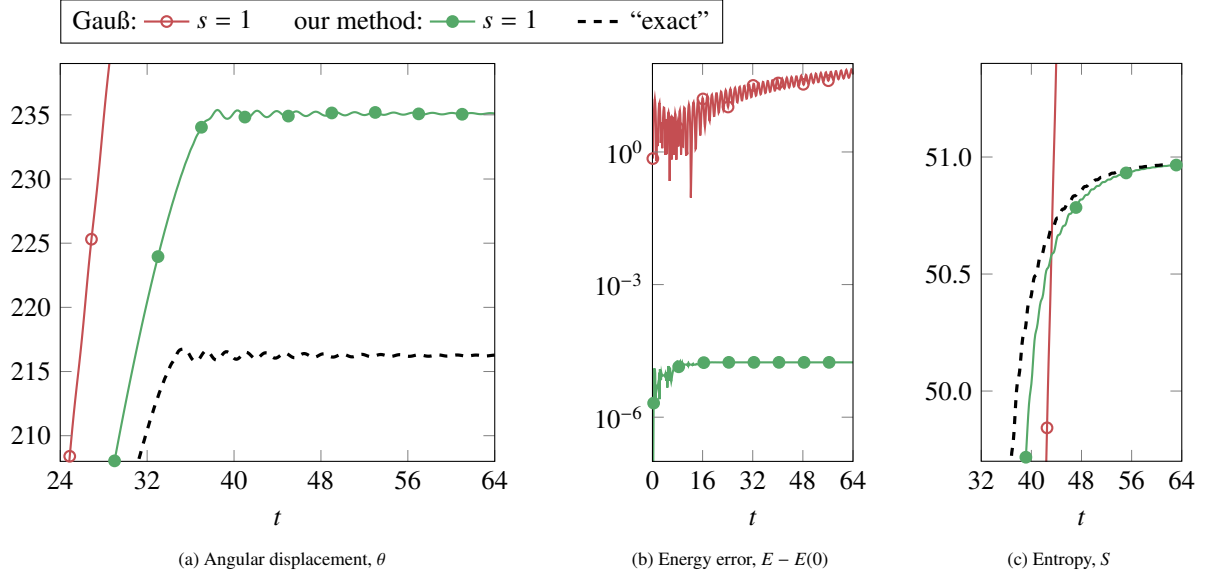


Figure 7: Evolution in θ , E , S for the combustion engine at $\Delta t_n = 2^{-3}$.

upon replacement of the finite-dimensional Euclidean space \mathbb{R}^d with a Banach space U . The GENERIC PDE is most conveniently stated in a variational form analogous to (26): find $u \in C^1(\mathbb{R}_+; U)$ satisfying known initial data, such that

$$M(u; \dot{u}, v) = B(u, w_E(u); v) + D(u, w_S(u); v) \quad (40)$$

for all test functions $v \in U$ and all times $t \in \mathbb{R}_+$, where $M : U \times U \times U \rightarrow \mathbb{R}$ is bilinear in its final two arguments, $B, D : U \times U \times U \rightarrow \mathbb{R}$ are each linear in the final argument v^3 with $B(u, \cdot; \cdot)$, $D(u, \cdot; \cdot)$ respectively skew-symmetric and positive-semidefinite (the Poisson and friction operators), and the functionals $E, S : U \rightarrow \mathbb{R}$ denote the energy and entropy. The functionals $w_E, w_S : U \rightarrow U$ are such that $M(u; \cdot, w_E(u)) = E'(u; \cdot)$, $M(u; \cdot, w_S(u)) = S'(u; \cdot)$, where E' , S' are the Fréchet derivatives of E, S respectively. Similar to (27), thermodynamic consistency imposes the conditions

$$B(u, \cdot; w_S(u)) = 0, \quad D(u, \cdot; w_E(u)) = 0. \quad (41)$$

We see these conditions ensure energy conservation ($\frac{d}{dt}E(\mathbf{x}) = 0$) and entropy generation ($\frac{d}{dt}S(\mathbf{x}) \geq 0$) along exact trajectories by considering $v = w_E(u)$ and $v = w_S(u)$ in (40); accordingly, $w_E(u)$ and $w_S(u)$ are the associated test functions for energy E and entropy S , which we shall introduce into our discretisation through auxiliary variables, i.e. projections \tilde{w}_E and \tilde{w}_S respectively onto a discrete test space. Similar to Theorem 3.1, for our construction of an energy- and entropy-stable integrator we assume access to certain extensions of B and D .

Assumption 4.1 (Characterisation of GENERIC operator compatibility). *Assume the existence of $\tilde{B}, \tilde{D} : U \times U \times U \times U \rightarrow \mathbb{R}$, linear in each of their final arguments, such that the following hold:*

1. *Consistency with B, D : for all u ,*

$$\tilde{B}(u, w_S(u), \cdot; \cdot) = B(u, \cdot; \cdot), \quad \tilde{D}(u, w_E(u), \cdot; \cdot) = D(u, \cdot; \cdot). \quad (42a)$$

2. *Skew-symmetry and positive semidefiniteness: for all $u, \tilde{w}_E, \tilde{w}_S \in U$, $\tilde{B}(u, \tilde{w}_S, \cdot; \cdot)$ is skew-symmetric, and $\tilde{D}(u, \tilde{w}_E, \cdot; \cdot)$ is positive-semidefinite.*

3. *Preservation of compatibility (41): for all $u, \tilde{w}_E, \tilde{w}_S \in U$,*

$$\tilde{B}(u, \tilde{w}_S, \cdot; \tilde{w}_S) = 0, \quad \tilde{D}(u, \tilde{w}_E, \cdot; \tilde{w}_E) = 0. \quad (42b)$$

³This is the significance of the semicolon. The GENERIC framework typically requires $B, D : U \times U \times U \rightarrow \mathbb{R}$ each be bilinear in their final two arguments, however this condition is not necessary for the construction of our energy- and entropy-preserving scheme.

With Theorem 4.1 in place, we follow a similar strategy to each of the ODE cases above to construct an energy- and entropy-stable integrator for (40), by (i) introducing auxiliary variables \tilde{w}_E and \tilde{w}_S approximating $w_E(u)$ and $w_S(u)$, and (ii) introducing these auxiliary variables into the right-hand side of (40). Discretising in space, let \mathbb{U} be a conforming finite-dimensional subspace of U , e.g. a finite element space. Defining the spacetime trial space for a given timestep

$$\mathbb{X}_n := \{ u \in \mathbb{P}_s(T_n; \mathbb{U}) \mid u(t_n) \text{ satisfies known initial data} \}, \quad (43)$$

our structure-preserving scheme is: find $(u, (\tilde{w}_E, \tilde{w}_S)) \in \mathbb{X}_n \times \dot{\mathbb{X}}_n^2$ such that for all $(v, (v_E, v_S)) \in \dot{\mathbb{X}}_n \times \dot{\mathbb{X}}_n^2$,

$$\mathcal{I}_n[M(u; \dot{u}, v)] = \mathcal{I}_n[\tilde{B}(u, \tilde{w}_S, \tilde{w}_E; v) + \tilde{D}(u, \tilde{w}_E, \tilde{w}_S; v)], \quad (44a)$$

$$\mathcal{I}_n[M(u; v_E, \tilde{w}_E)] = \int_{T_n} E'(u; v_E), \quad (44b)$$

$$\mathcal{I}_n[M(u; v_S, \tilde{w}_S)] = \int_{T_n} S'(u; v_S). \quad (44c)$$

By (42a) we see (44a) identifies with the original weak formulation (40) when $(\tilde{w}_E, \tilde{w}_S) = (w_E(u), w_S(u))$.

Theorem 4.2 (Energy and entropy stability of (44)). *Assuming solutions exist, the integrator (44) is energy- and entropy-stable, with $E(u(t_{n+1})) = E(u(t_n))$ and $S(u(t_{n+1})) \geq S(u(t_n))$.*

Proof. By considering respectively $v_E = \dot{u}$, $v_S = \dot{u}$ and $v = \tilde{w}_E$, $v = \tilde{w}_S$ in (44),

$$\begin{aligned} E(u(t_{n+1})) - E(u(t_n)) &= \int_{T_n} \dot{E} \\ &= \int_{T_n} E'(u; \dot{u}) \\ &= \mathcal{I}_n[M(u; \dot{u}, \tilde{w}_E)] \\ &= \mathcal{I}_n \left[\begin{array}{c} \tilde{B}(u, \tilde{w}_S, \tilde{w}_E; \tilde{w}_E) \\ + \tilde{D}(u, \tilde{w}_E, \tilde{w}_S; \tilde{w}_E) \end{array} \right] \\ &= 0, \end{aligned} \quad \begin{aligned} S(u(t_{n+1})) - S(u(t_n)) &= \int_{T_n} \dot{S} \\ &= \int_{T_n} S'(u; \dot{u}) \\ &= \mathcal{I}_n[M(u; \dot{u}, \tilde{w}_S)] \\ &= \mathcal{I}_n \left[\begin{array}{c} \tilde{B}(u, \tilde{w}_S, \tilde{w}_E; \tilde{w}_S) \\ + \tilde{D}(u, \tilde{w}_E, \tilde{w}_S; \tilde{w}_S) \end{array} \right] \\ &\geq 0, \end{aligned} \quad (45a)$$

$$\begin{aligned} &= \int_{T_n} E'(u; \dot{u}) \\ &= \mathcal{I}_n[M(u; \dot{u}, \tilde{w}_S)] \end{aligned} \quad (45b)$$

$$\begin{aligned} &= \mathcal{I}_n \left[\begin{array}{c} \tilde{B}(u, \tilde{w}_S, \tilde{w}_E; \tilde{w}_S) \\ + \tilde{D}(u, \tilde{w}_E, \tilde{w}_S; \tilde{w}_S) \end{array} \right] \end{aligned} \quad (45c)$$

$$\begin{aligned} &= \mathcal{I}_n \left[\begin{array}{c} \tilde{B}(u, \tilde{w}_S, \tilde{w}_E; \tilde{w}_S) \\ + \tilde{D}(u, \tilde{w}_E, \tilde{w}_S; \tilde{w}_S) \end{array} \right] \end{aligned} \quad (45d)$$

$$\begin{aligned} &= 0, \\ &\geq 0, \end{aligned} \quad (45e)$$

where the final equality and inequality hold by Theorem 4.1. \square

Remark 4.3. *Unlike in the finite-dimensional cases above, the auxiliary variables \tilde{w}_E , \tilde{w}_S generally cannot be eliminated. The additional cost incurred in solving for them is nontrivial.*

4.1. Boltzmann equation

The Boltzmann equation is a key example of a GENERIC PDE. We consider the nondimensionalised Boltzmann equation in $d \geq 1$ dimensions,

$$\dot{f} = -\mathbf{v} \cdot \nabla_{\mathbf{x}} f + \nabla_{\mathbf{x}} \phi \cdot \nabla_{\mathbf{v}} f + \frac{1}{\text{Kn}} C(f). \quad (46)$$

Here $f(\mathbf{x}, \mathbf{v}, t) \in \mathbb{R}$ represents the particle density function in the position and velocity $\mathbf{x}, \mathbf{v} \in \mathbb{R}^d$, $\nabla_{\mathbf{x}}$ and $\nabla_{\mathbf{v}}$ denote the partial derivatives with respect to \mathbf{x} and \mathbf{v} , $\phi(\mathbf{x}) \in \mathbb{R}$ represents a potential energy density, and Kn is the Knudsen number. The term C denotes the Boltzmann collision operator, defined by

$$C(f) := \int_{\mathbf{v}^*, \mathbf{n} \in S^{d-1}} \beta(\theta, \|\mathbf{g}\|) (f^\dagger f^{*\dagger} - f f^*) d\mathbf{v}^* d\mathbf{n}. \quad (47)$$

Here $\mathbf{g} := \mathbf{v} - \mathbf{v}^*$ is the relative velocity, \mathbf{n} is the collision normal (on the unit $(d-1)$ -sphere $S^{d-1} \subset \mathbb{R}^n$), $\theta = 2\angle(\mathbf{g}, \mathbf{n})$ is the scattering angle, and $\beta(\theta, \|\mathbf{g}\|) \geq 0$ is the collision kernel where $\|\cdot\|$ denotes the ℓ^2 norm; the fields f^* , f^\dagger , $f^{*\dagger}$ are shorthand for

$$f^* = f|_{\mathbf{v}=\mathbf{v}^*}, \quad f^\dagger = f|_{\mathbf{v}=\mathbf{v}^\dagger}, \quad f^{*\dagger} = f|_{\mathbf{v}=\mathbf{v}^{*\dagger}}, \quad (48a)$$

where in turn $\mathbf{v}^\dagger, \mathbf{v}^{*\dagger}$ are the unique post-collision velocities (see Figure 8) satisfying

$$\mathbf{v} + \mathbf{v}^* = \mathbf{v}^\dagger + \mathbf{v}^{*\dagger}, \quad \frac{1}{2}\|\mathbf{v}\|^2 + \frac{1}{2}\|\mathbf{v}^*\|^2 = \frac{1}{2}\|\mathbf{v}^\dagger\|^2 + \frac{1}{2}\|\mathbf{v}^{*\dagger}\|^2, \quad \mathbf{n} = \frac{\mathbf{v} - \mathbf{v}^\dagger}{\|\mathbf{v} - \mathbf{v}^\dagger\|}. \quad (48b)$$

We assume periodic boundary conditions in \mathbf{x} , and a vanishing asymptotic boundary condition in \mathbf{v} of $f \rightarrow 0$ as $\|\mathbf{v}\| \rightarrow \infty$. The Boltzmann equation (46) has a conserved energy E and generated entropy S ,

$$E := \int_{\mathbf{x}, \mathbf{v}} \left(\frac{1}{2}\|\mathbf{v}\|^2 + \phi \right) f, \quad S := \int_{\mathbf{x}, \mathbf{v}} (1 - \log f) f. \quad (49)$$

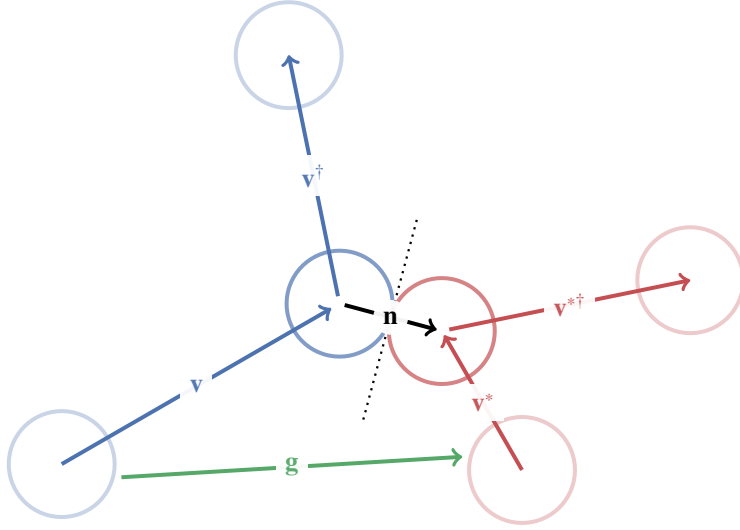


Figure 8: Illustration of the relationship between the velocities $\mathbf{v}, \mathbf{v}^*, \mathbf{v}^\dagger, \mathbf{v}^{*\dagger}$, and collision normal \mathbf{n} .

To handle the asymptotic boundary conditions in \mathbf{v} , we parametrise f as

$$f(\mathbf{x}, \mathbf{v}, t) = f_0(\mathbf{v}) \exp(u(\mathbf{x}, \mathbf{v}, t)) \quad (50)$$

for u in some sufficiently regular function space U . The function $f_0 > 0$ characterises the asymptotic behaviour in \mathbf{v} , with $f_0 \rightarrow 0$ and $u = o[\log f_0]$ as $\|\mathbf{v}\| \rightarrow \infty$. Note then that $\dot{f} = f\dot{u}$.

To apply the scheme (44) to construct an energy- and entropy-stable integrator for (46), we recall the formulation of the Boltzmann equation in the GENERIC formalism presented by Öttinger [21].

We first cast (46) into a variational form. By testing against $v \in U$ and after some classical manipulation of the collision term, we arrive at the following: find $u \in C^1(\mathbb{R}_+; U)$ satisfying known initial data, such that

$$\int_{\mathbf{x}, \mathbf{v}} f \dot{u} v = \int_{\mathbf{x}, \mathbf{v}} (\nabla_{\mathbf{x}} \phi \cdot \nabla_{\mathbf{v}} v - \mathbf{v} \cdot \nabla_{\mathbf{x}} v) f + \frac{1}{4Kn} \int_{\mathbf{x}, \mathbf{v}, \mathbf{v}^*, \mathbf{n}} \beta (f^\dagger f^{*\dagger} - f f^*) (v + v^* - v^\dagger - v^{*\dagger}) \quad (51)$$

at all times $t \in \mathbb{R}_+$ and for all $v \in U$, where $v^*, v^\dagger, v^{*\dagger}$ are defined analogously to $f^*, f^\dagger, f^{*\dagger}$ as in (48a). This induces the choice of the left-hand side operator $M : U \times U \times U \rightarrow \mathbb{R}$,

$$M(u; w, v) := \int_{\mathbf{x}, \mathbf{v}} f w v = \int_{\mathbf{x}, \mathbf{v}} f_0 \exp(u) w v. \quad (52)$$

Now, consider the energy E and entropy S (49) as functions in u . These have Fréchet derivatives

$$E'(u; \delta u) = \int_{\mathbf{x}, \mathbf{v}} \left(\frac{1}{2}\|\mathbf{v}\|^2 + \phi \right) f \delta u, \quad S'(u; \delta u) = - \int_{\mathbf{x}, \mathbf{v}} f \log f \delta u, \quad (53)$$

where again f is defined in terms of u by (50). Seeking $w_E(u)$, $w_S(u)$ such that $M(u; \cdot, w_E(u)) = E'(u; \cdot)$, $M(u; \cdot, w_S(u)) = S'(u; \cdot)$, the solution is immediate:

$$w_E(u) = \frac{1}{2} \|\mathbf{v}\|^2 + \phi, \quad w_S(u) = -\log f. \quad (54)$$

Up to a constant factor in w_S , these align with [21, eqs. (6, 7)]. Define the Poisson and friction operators $B, D : U \times U \times U \rightarrow \mathbb{R}$,

$$B(u, \tilde{w}_E; v) := \int_{\mathbf{x}, \mathbf{v}} (\nabla_{\mathbf{x}} \tilde{w}_E \cdot \nabla_{\mathbf{v}} v - \nabla_{\mathbf{v}} \tilde{w}_E \cdot \nabla_{\mathbf{x}} v) f, \quad (55a)$$

$$D(u, \tilde{w}_S; v) := \frac{1}{4\text{Kn}} \int_{\mathbf{x}, \mathbf{v}, \mathbf{v}^*, \mathbf{n}} \beta \left(\exp(-\tilde{w}_S^\dagger - \tilde{w}_S^{*\dagger}) - \exp(-\tilde{w}_S - \tilde{w}_S^*) \right) (v + v^* - v^\dagger - v^{*\dagger}), \quad (55b)$$

where \tilde{w}_S^* , \tilde{w}_S^\dagger , $\tilde{w}_S^{*\dagger}$ are again defined analogously to f^* , f^\dagger , $f^{*\dagger}$ (48a) and v^* , v^\dagger , $v^{*\dagger}$ (48b). The Poisson operator B in (55a) aligns immediately with the operator L as defined in [21, eq. (8)]. The skew-symmetry of B is immediate, while the positive-definiteness of D relies on the observation that $(e^{-x} - e^{-y})(y - x) \geq 0$. The GENERIC compatibility condition $B(u, \cdot; w_S) = 0$ holds after algebraic simplification, while $D(u, \cdot; w_E) = 0$ can be seen from the conservation of energy condition $\frac{1}{2} \|\mathbf{v}\|^2 + \frac{1}{2} \|\mathbf{v}^*\|^2 = \frac{1}{2} \|\mathbf{v}^\dagger\|^2 + \frac{1}{2} \|\mathbf{v}^{*\dagger}\|^2$ (48b). With M, B, D as defined, the Boltzmann equation is a GENERIC PDE of the form (40); we can thus apply (44) to preserve the energy and entropy stability, if we can properly define suitable $\tilde{B}, \tilde{D} : U \times U \times U \times U \rightarrow \mathbb{R}$ to satisfy Theorem 4.1.

Take \tilde{w}_E, \tilde{w}_S to be approximations to $w_E(u), w_S(u)$. The incorporation of \tilde{w}_S into B is simple, with \tilde{B} defined

$$\tilde{B}(u, \tilde{w}_S; \tilde{w}_E, v) := \int_{\mathbf{x}, \mathbf{v}} (\nabla_{\mathbf{x}} \tilde{w}_E \cdot \nabla_{\mathbf{v}} v - \nabla_{\mathbf{v}} \tilde{w}_E \cdot \nabla_{\mathbf{x}} v) \exp(-\tilde{w}_S). \quad (56)$$

In the case of $\tilde{w}_S = w_S(u) = -\log f$, we see this identifies with B as $\exp(-\tilde{w}_S) = \exp(\log f) = f$; we see \tilde{B} evaluates to 0 for $v = \tilde{w}_S$ by the substitution $\exp(-\tilde{w}_S) \nabla \tilde{w}_S = -\nabla[\exp(-\tilde{w}_S)]$ and integration by parts in \mathbf{x}, \mathbf{v} noting the periodic boundary conditions and assuming $\tilde{w}_S \rightarrow \infty$ as $\|\mathbf{v}\| \rightarrow \infty$ such that $\exp(-\tilde{w}_S) \rightarrow 0$.

The incorporation of \tilde{w}_E into D is somewhat more involved, and requires rewriting (55b). Let $\Sigma \subset \mathbb{R}^3 \times (\mathbb{R}^3)^4$ denote the manifold of tuples $(\mathbf{x}, (\mathbf{v}, \mathbf{v}^*, \mathbf{v}^\dagger, \mathbf{v}^{*\dagger}))$ satisfying the relations (48b) characterising all possible collisions; the final relation in (48b) now instead serves as a definition for $\mathbf{n} = \frac{\mathbf{v} - \mathbf{v}^\dagger}{\|\mathbf{v} - \mathbf{v}^\dagger\|}$ and consequently $\theta = 2\angle(\mathbf{g}, \mathbf{n})$. We endow Σ with the metric induced from $\mathbb{R}^3 \times (\mathbb{R}^3)^4$. The friction operator D may then be written as an integral over Σ ,

$$D(u; \tilde{w}_S, v) := \frac{1}{4\text{Kn}} \int_{\Sigma} \beta \left(\exp(-\tilde{w}_S^\dagger - \tilde{w}_S^{*\dagger}) - \exp(-\tilde{w}_S - \tilde{w}_S^*) \right) (v + v^* - v^\dagger - v^{*\dagger}). \quad (57)$$

This formulation of the friction operator aligns with [21, eq. (12)], up to a minor modification made by Öttinger to enforce linearity⁴.

With this reformulation, we may define an auxiliary manifold $\tilde{\Sigma} \subset \mathbb{R}^3 \times (\mathbb{R}^3)^4$ of tuples $(\mathbf{x}, (\mathbf{v}, \mathbf{v}^*, \mathbf{v}^\dagger, \mathbf{v}^{*\dagger}))$ satisfying the auxiliary relations

$$\mathbf{v} + \mathbf{v}^* = \mathbf{v}^\dagger + \mathbf{v}^{*\dagger}, \quad \tilde{w}_E|_{\mathbf{v}=\mathbf{v}} + \tilde{w}_E|_{\mathbf{v}=\mathbf{v}^*} = \tilde{w}_E|_{\mathbf{v}=\mathbf{v}^\dagger} + \tilde{w}_E|_{\mathbf{v}=\mathbf{v}^{*\dagger}}, \quad (58a)$$

which we again endow with the metric induced from $\mathbb{R}^3 \times (\mathbb{R}^3)^4$. Similarly to $f^*, f^\dagger, f^{*\dagger}$ as in (48a) we take $\psi^*, \psi^\dagger, \psi^{*\dagger}$, for an arbitrary function ψ in \mathbf{v} , as shorthand for

$$\psi^* := \psi|_{\mathbf{v}=\mathbf{v}^*}, \quad \psi^\dagger := \psi|_{\mathbf{v}=\mathbf{v}^\dagger}, \quad \psi^{*\dagger} := \psi|_{\mathbf{v}=\mathbf{v}^{*\dagger}}. \quad (58b)$$

We may then introduce \tilde{w}_E into the definition of \tilde{D} implicitly through $\tilde{\Sigma}$:

$$\tilde{D}(u, \tilde{w}_E; \tilde{w}_S, v) := \frac{1}{4\text{Kn}} \int_{\tilde{\Sigma}} \beta \left(\exp(-\tilde{w}_S^\dagger - \tilde{w}_S^{*\dagger}) - \exp(-\tilde{w}_S - \tilde{w}_S^*) \right) (v + v^* - v^\dagger - v^{*\dagger}). \quad (59)$$

⁴This modification is unnecessary for our purposes as the structure-preserving properties hold regardless. Öttinger [21] characterises both the collision kernel β and the manifold of admissible collisions Σ through a single distribution function w of transition probabilities supported on Σ .

Considering $\tilde{w}_E = w_E(u) = \frac{1}{2}\|\mathbf{v}\|^2 + \phi(\mathbf{x})$, we see this identifies with D as the conditions (58a) on $\mathbf{v}, \mathbf{v}^*, \mathbf{v}^\dagger, \mathbf{v}^{*\dagger}$ align with those on $\mathbf{v}, \mathbf{v}^*, \mathbf{v}^\dagger, \mathbf{v}^{*\dagger}$ (48b); we see \tilde{D} evaluates to zero for $v = \tilde{w}_E$ as the conditions (58a) on $\mathbf{v}^*, \mathbf{v}^\dagger, \mathbf{v}^{*\dagger}$ imply $\tilde{w}_E + \tilde{w}_E^* - \tilde{w}_E^\dagger - \tilde{w}_E^{*\dagger} = 0$ on $\tilde{\Sigma}$.

For a finite-dimensional subspace $\mathbb{U} \subset U$ and discrete space-time function space \mathbb{X}_n defined as in (43)⁵, we finally derive the following energy- and entropy-stable scheme for the Boltzmann equation (46): find $(u, (\tilde{w}_E, \tilde{w}_S)) \in \mathbb{X}_n \times \tilde{\mathbb{X}}_n^2$ such that for all $(v, (v_E, v_S)) \in \tilde{\mathbb{X}}_n \times \tilde{\mathbb{X}}_n^2$,

$$\mathcal{I}_n \left[\int_{\mathbf{x}, \mathbf{v}} f \dot{u} v \right] = \mathcal{I}_n \left[\int_{\mathbf{x}, \mathbf{v}} (\nabla_{\mathbf{x}} \tilde{w}_E \cdot \nabla_{\mathbf{v}} v - \nabla_{\mathbf{v}} \tilde{w}_E \cdot \nabla_{\mathbf{x}} v) \tilde{f} + \frac{1}{4\text{Kn}} \int_{\tilde{\Sigma}} \beta (\tilde{f}^\dagger \tilde{f}^{*\dagger} - \tilde{f} \tilde{f}^*) (v + v^* - v^\dagger - v^{*\dagger}) \right], \quad (60a)$$

$$\mathcal{I}_n \left[\int_{\mathbf{x}, \mathbf{v}} f \tilde{w}_E v_E \right] = \int_{T_n} \int_{\mathbf{x}, \mathbf{v}} f \left(\frac{1}{2} \|\mathbf{v}\|^2 + \phi(\mathbf{x}) \right) v_E, \quad (60b)$$

$$\mathcal{I}_n \left[\int_{\mathbf{x}, \mathbf{v}} f \tilde{w}_S v_S \right] = - \int_{T_n} \int_{\mathbf{x}, \mathbf{v}} f \log f v_S, \quad (60c)$$

where again f is defined as in (50), the auxiliary density function \tilde{f} is shorthand for $\tilde{f} := \exp(-\tilde{w}_S)$, the functions $\tilde{f}^*, \tilde{f}^\dagger, \tilde{f}^{*\dagger}$ and $v^*, v^\dagger, v^{*\dagger}$ are defined via (58b) for $\mathbf{v}^*, \mathbf{v}^\dagger, \mathbf{v}^{*\dagger}$ defined as in (58a), and $\tilde{\Sigma} \subset \mathbb{R}^3 \times (\mathbb{R}^3)^4$ is the auxiliary manifold of $(\mathbf{x}, (\mathbf{v}, \mathbf{v}^*, \mathbf{v}^\dagger, \mathbf{v}^{*\dagger}))$ satisfying (58a).

As in the proof of Theorem 4.2, the conservation of E and dissipation of S can then be shown by testing with $(v, v_E) = (\tilde{w}_E, \dot{u})$ and $(v, v_S) = (\tilde{w}_S, \dot{u})$ respectively.

Remark 4.4. *Practical implementation of the integral over the auxiliary manifold $\tilde{\Sigma}$ in \tilde{D} would in general be difficult. However, under certain assumptions on the space \mathbb{U} , this problem reduces to one only as difficult as evaluating D (55b), as we now describe.*

Suppose \mathbb{U} , itself a finite-dimensional space over (\mathbf{x}, \mathbf{v}) , is chosen to be the tensor product $\mathbb{U}_{\mathbf{x}} \otimes \mathbb{U}_{\mathbf{v}}$ of finite-dimensional spaces over \mathbf{x} and \mathbf{v} respectively. If both $\phi \in \mathbb{U}_{\mathbf{x}}$ and $\frac{1}{2}\|\mathbf{v}\|^2 \in \mathbb{U}_{\mathbf{v}}$ (e.g. with $\mathbb{U}_{\mathbf{v}}$ a degree-2 finite-element space), then $w_E = \frac{1}{2}\|\mathbf{v}\|^2 + \phi$ is element of \mathbb{U} , and consequently an element too of $\tilde{\mathbb{X}}_n$ by time independence. Choosing the quadrature rule $\mathcal{I}_n = \int_{T_n}$ (i.e. such that the scheme (60) is a structure-preserving modification of a continuous Petrov–Galerkin scheme) we see that (60b) is then solved exactly by $\tilde{w}_E = w_E \in \tilde{\mathbb{X}}_n$. The auxiliary variable \tilde{w}_E may then be eliminated, and \tilde{D} coincides with D .

4.2. Benjamin–Bona–Mahony equation

In this section we consider the Benjamin–Bona–Mahony (BBM) equation [22] in $u : \mathbb{R}_+ \times \Omega \rightarrow \mathbb{R}$ over an interval $\Omega \subset \mathbb{R}$,

$$\dot{u} - \partial_x^2 \dot{u} = -\partial_x u - u \partial_x u, \quad (61)$$

where ∂_x denotes the partial derivative with respect to the spatial coordinate x . We impose periodic boundary conditions. We shall observe that long-time (conservative) simulations of (61) using the simplification of (44) exhibit substantially better physical fidelity compared to a (symplectic) Gauß scheme of the same order with the same spatial discretisation.

The BBM equation is a Hamiltonian system with a conserved energy (denoted here by H in place of E)

$$H(u) := \int_{\Omega} \frac{1}{2} u^2 + \frac{1}{6} u^3, \quad (62)$$

and has exactly two other independent invariants:

$$I_1(u) := \int_{\Omega} u, \quad I_2(u) := \int_{\Omega} u^2 + u_x^2. \quad (63)$$

⁵Since the Boltzmann equation has a hyperbolic nature, a non-conforming space and \mathbb{U} and corresponding non-conforming modification to (60) may be more effective in practice.

To apply the scheme (44) to construct an energy-stable integrator for (61), we must first show (61) may be written in the form (40).

A typical semidiscrete variational form of (61) can be found by testing in the L^2 inner product against some test function v , and applying integration by parts: find $u \in C^1(\mathbb{R}_+; U)$ satisfying known initial data such that

$$(\dot{u} - \partial_x^2 \dot{u}, v) = -(\partial_x u + u \partial_x u, v) \implies (\dot{u}, v) + (\partial_x \dot{u}, \partial_x v) = -(\partial_x [u + \frac{1}{2} u^2], v) \implies (\dot{u}, v)_{H^1} = (u + \frac{1}{2} u^2, \partial_x v) \quad (64)$$

at all times $t \in \mathbb{R}_+$ and for all $v \in U$. We thus take M to be the H^1 inner product of the final two arguments. The associated test function $w_H(u)$ for H must then satisfy

$$(\cdot, w_H(u))_{H^1} = H'(u; \cdot) \implies (\cdot, w_H(u) - \partial_x^2 w_H(u)) = (u + \frac{1}{2} u^2, \cdot), \quad (65)$$

implying $w_H(u)$ is implicitly defined in strong form to satisfy

$$w_H(u) - \partial_x^2 w_H(u) = u + \frac{1}{2} u^2. \quad (66)$$

We may therefore write our semidiscrete variational form (64) in terms of $w_H(u)$ as

$$(\dot{u}, v)_{H^1} = (w_H(u) - \partial_x^2 w_H(u), \partial_x v) \quad (67a)$$

$$= \frac{1}{2} [(w_H(u), \partial_x v) + (\partial_x w_H(u), \partial_x^2 v) - (\partial_x w_H(u), v) - (\partial_x^2 w_H(u), \partial_x v)], \quad (67b)$$

$$= \frac{1}{2} [(w_H(u), \partial_x v)_{H^1} - (\partial_x w_H(u), v)_{H^1}]. \quad (67c)$$

Defining skew-symmetric $B(w, v) := \frac{1}{2} [(w, \partial_x v)_{H^1} - (\partial_x w, v)_{H^1}]$ (independent of u) and setting $D = 0$, this aligns with the GENERIC format (40).

For a chosen (twice weakly-differentiable) discrete space $\mathbb{U} \subset H^2(\Omega)^6$, we may therefore use our general structure-preserving integrator (44) to derive the following energy-conserving scheme: find $(u, \tilde{w}_H) \in \mathbb{X}_n \times \mathbb{X}_n$ such that

$$\mathcal{I}_n[(\dot{u}, v)_{H^1}] = \frac{1}{2} \mathcal{I}_n[(\tilde{w}_H, \partial_x v)_{H^1} - (\partial_x \tilde{w}_H, v)_{H^1}], \quad (68a)$$

$$\mathcal{I}_n[(v_H, \tilde{w}_H)_{H^1}] = \int_{T_n} (u + \frac{1}{2} u^2, v_H), \quad (68b)$$

for all $(v, v_H) \in \mathbb{X}_n \times \mathbb{X}_n$. Again, taking $(v, v_H) = (\tilde{w}_H, \dot{u})$ confirms that (68) conserves H .

4.2.1. Numerical test

We simulate the very-long-time behaviour of a soliton to verify and motivate these conservation properties. We consider the domain $\Omega = (-50, 50)$. Up to projection, the following ICs form a soliton⁷ of speed $\frac{1+\sqrt{5}}{2}$:

$$u(0) = \frac{3\sqrt{5}-3}{2} \operatorname{sech}\left(\frac{\sqrt{5}-1}{4}x\right)^2, \quad (69)$$

where sech is the hyperbolic secant function. Over an interval mesh of uniform mesh width 2, we take \mathbb{U} to be the (degree-3) Hermite space (see Ern & Guermond [24, Chap. 5]); in time, we take a uniform timestep $\Delta t_n = 1$. Under these conditions, we compare the results from a 2-stage (symplectic) Gauß method as applied to (64) with that of the scheme (68) with \mathcal{I}_n the exact integral⁸ and $s = 2$.

Figure 9 shows the evolution of the energy $H(u)$ under both schemes. Artificial dissipation in the energy with the Gauß method causes the value to decrease from its initial value of around 11.1 to around 6.2 at the final time $t = 2 \cdot 10^4$.

⁶With appropriate handling of arising facet terms, it is similarly possible to derive an energy-stable integrator that only requires the lower regularity $\mathbb{U} \subset H^1(\Omega)$.

⁷The appropriate notion of a nonlinear wave under periodic boundary conditions is not a soliton, but a cnoidal wave (see Ablowitz & Segur [23, Sec. 2.3]). The value of the ICs at the boundary $x = \pm 50$ however are approximately 2×10^{-13} , implying this distinction on this domain is negligible, especially after projection into the discrete space \mathbb{U} .

⁸We are able to compute this exactly, as all terms in the discretisation (68) are polynomial.

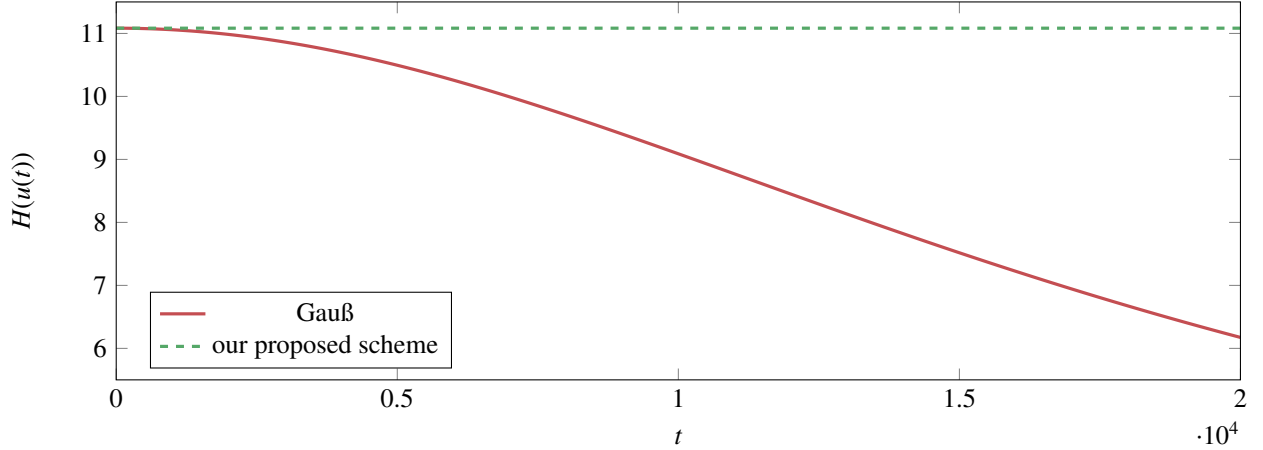


Figure 9: Evolution of the energy $H(u)$ when solving the BBM equations with a Gauß method and our proposed scheme (68).

Figure 10 shows u approximated with both schemes at various times along the simulation. The dissipation in $H(u)$ with the Gauß method correlates with a reduction in the amplitude of u , causing the speed of the soliton to decrease. At $t = 2 \times 10^4$, the soliton in the Gauß simulation has speed approximately 1.45; compare with the exact value of approximately 1.618, and that of the numerical solution from our proposed scheme of approximately 1.617.

Of note is the conservation of the further invariant $I_2(u)$ (63) i.e. the squared H^1 norm $\|u\|_{H^1}^2$. Figure 11 shows the evolution of $I_2(u)$ under our proposed scheme. While the construction of the scheme (68) does not guarantee the discrete conservation of $I_2(u)$, we find numerically that $I_2(u(t_n))$ oscillates within the small interval (15.9660, 15.9667) over the simulation duration; this is reminiscent of the approximate conservation of energy exhibited by symplectic integrators (see Figure 2a or e.g. [12, Chap. I, Fig 4.1]). The proof of this property remains an open problem. Conversely, as the Gauß method conserves $I_2(u)$, reductions in the L^2 norm of u due to the decreasing energy $H(u)$ must induce increases in its H^1 seminorm; this manifests as the undesirable oscillations seen throughout the domain in Figure 10. No such oscillations are observed with our proposed scheme.

5. Conclusions

In this work we have built upon our framework [3] to devise conservative numerical integrators for systems of ODEs with multiple invariants, and energy- and entropy-stable integrators for ODEs and PDEs in the GENERIC formalism.

We mention two natural questions arising from this work. The first lies in the consideration of multiply dissipative PDEs: is it possible to use the auxiliary variable framework to preserve arbitrarily many dissipation structures for dissipative systems of ODEs or PDEs? The second lies in the construction of conservative integrators for multiply conservative PDEs. Casting such equations into a semidiscrete form (discretising in space only), one retrieves a sparsely coupled system of ODEs. Our conservative integrator for multiply conservative ODEs (14) could in theory be applied to this ODE system to retrieve a conservative discretisation of the original PDE. However, there is no guarantee that the alternating form construction in Section 2 (Theorem 2.3) would not damage the sparsity pattern of the system. Is it possible to conserve arbitrarily many invariants in multi-conservative PDE systems, without breaking the sparsity structure?

6. Code availability

The code used for the numerical results employed Firedrake [25], PETSc [26], and MUMPS [27]. All code for reproducing the numerical results of this work and major Firedrake components have been archived at [28].

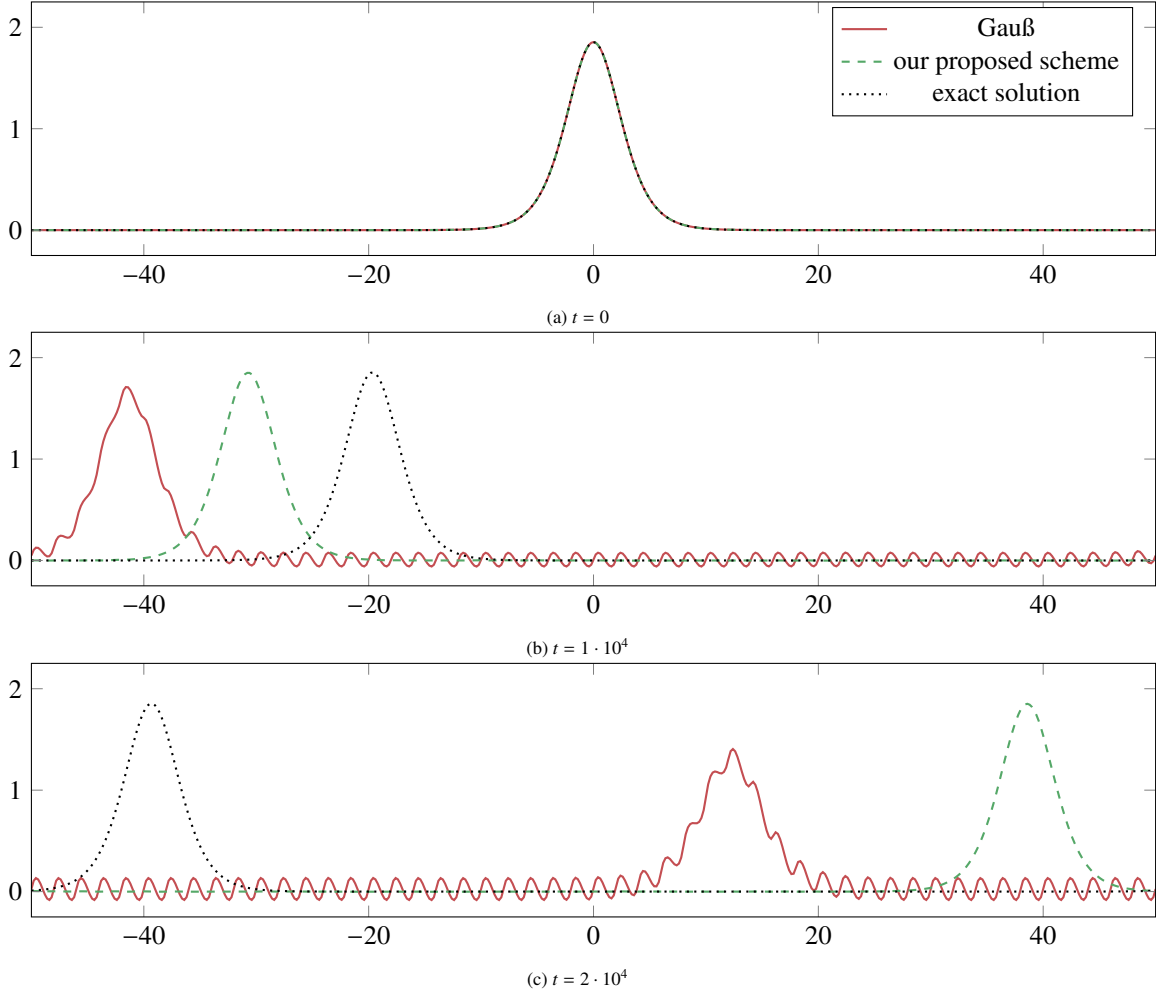


Figure 10: Plots of $u(x)$ in the BBM simulations using a Gauß method and our proposed scheme at times $t \in \{0, 1 \cdot 10^4, 2 \cdot 10^4\}$. The exact solution is included for comparison. The results with the Gauß method exhibit incorrect wave speeds and oscillations throughout the domain; the results with our proposed scheme exhibit no such oscillations, and a wave speed accurate to three digits.

Acknowledgments

This work was funded by the European Union [ERC, GeoFEM, 101164551], the Engineering and Physical Sciences Research Council (EPSRC) [grant numbers EP/R029423/1 and EP/W026163/1], the EPSRC Energy Programme [grant number EP/W006839/1], a CASE award from the UK Atomic Energy Authority, the Donatio Universitatis Carolinae Chair “Mathematical modelling of multicomponent systems”, and the UKRI Digital Research Infrastructure Programme through the Science and Technology Facilities Council’s Computational Science Centre for Research Communities (CoSeC). Views and opinions expressed are however those of the authors only and do not necessarily reflect those of the European Union or the European Research Council. Neither the European Union nor the granting authority can be held responsible for them. For the purpose of open access, the authors have applied a CC BY public copyright licence to any author accepted manuscript arising from this submission. No new data were generated or analysed during this study.

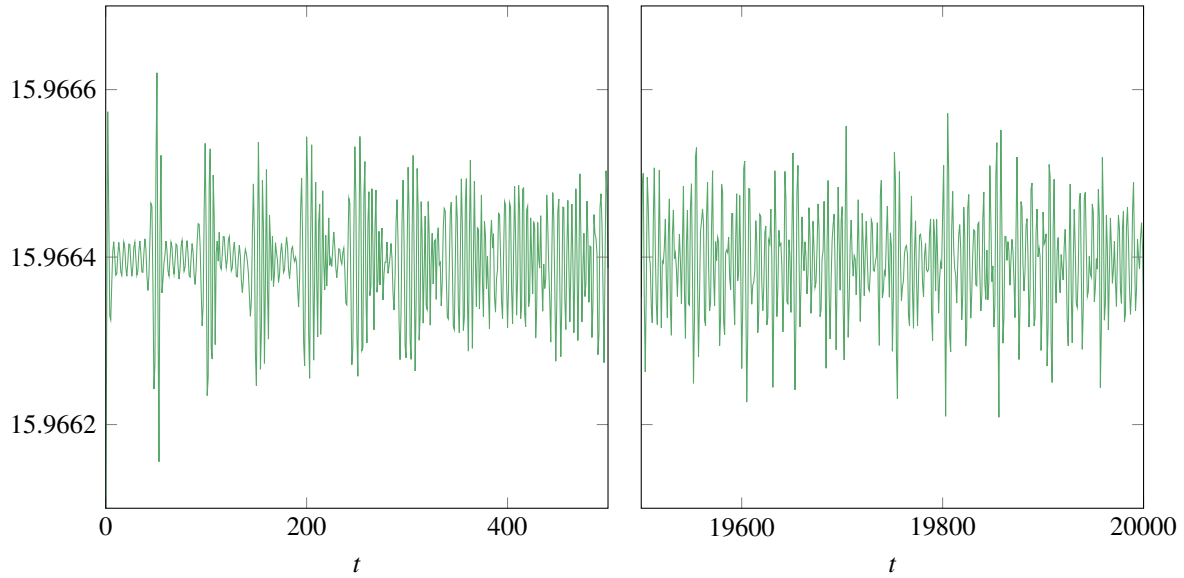


Figure 11: Evolution of the H^1 norm $\|u\|_{H^1}$ when solving the BBM equations with our proposed scheme.

References

- [1] E. Hairer, M. Hochbruck, A. Iserles, C. Lubich, Geometric numerical integration, Oberwolfach Reports 3 (1) (2006) 805–882. doi:10.4171/owr/2006/14.
- [2] Z. Ge, J. E. Marsden, Lie–Poisson Hamilton–Jacobi theory and Lie–Poisson integrators, Physics Letters A 133 (3) (1988) 134–139. doi:10.1016/0375-9601(88)90773-6.
- [3] B. D. Andrews, P. E. Farrell, High-order conservative and accurately dissipative numerical integrators via auxiliary variables, SIAM Journal on Scientific Computing (2025). doi:10.1137/25M1756673.
- [4] M. Grmela, H. C. Öttinger, Dynamics and thermodynamics of complex fluids. I. Development of a general formalism, Physical Review E 56 (6) (1997) 6620–6632. doi:10.1103/PhysRevE.56.6620.
- [5] H. C. Öttinger, M. Grmela, Dynamics and thermodynamics of complex fluids. II. Illustrations of a general formalism, Physical Review E 56 (6) (1997) 6633–6655. doi:10.1103/PhysRevE.56.6633.
- [6] D. Cohen, E. Hairer, Linear energy-preserving integrators for Poisson systems, BIT Numerical Mathematics 51 (1) (2011) 91–101. doi:10.1007/s10543-011-0310-z.
- [7] L. Brugnano, F. Iavernaro, Line integral methods which preserve all invariants of conservative problems, Journal of Computational and Applied Mathematics 236 (16) (2012) 3905–3919. doi:10.1016/j.cam.2012.03.026.
- [8] L. Brugnano, F. Iavernaro, Line integral methods for conservative problems, CRC Press, Boca Raton, FL, United States, 2016. doi:10.1201/b19319.
- [9] L. Brugnano, G. Frasca-Caccia, F. Iavernaro, Line integral solution of Hamiltonian PDEs, Mathematics 7 (3) (2019) 275. doi:10.3390/math7030275.
- [10] I. Romero, Thermodynamically consistent time-stepping algorithms for non-linear thermomechanical systems, International Journal for Numerical Methods in Engineering 79 (6) (2009) 706–732. doi:10.1002/nme.2588.
- [11] J. Giesselmann, A. Karsai, T. Tscherpel, Energy-consistent Petrov–Galerkin time discretization of port-Hamiltonian systems, SMAI Journal of Computational Mathematics 11 (2025) 335–367. doi:10.5802/smai-jcm.127.

- [12] E. Hairer, C. Lubich, G. Wanner, Geometric numerical integration: structure-preserving algorithms for ordinary differential equations, Springer Science & Business Media, Heidelberg, Germany, 2006. doi:10.1007/3-540-30666-8.
- [13] A. Ern, J.-L. Guermond, Finite elements III: first-order and time-dependent PDEs, Vol. 74 of Texts in Applied Mathematics, Springer International Publishing, Cham, Switzerland, 2021. doi:10.1007/978-3-030-57348-5.
- [14] R. I. McLachlan, G. R. W. Quispel, N. Robidoux, Geometric integration using discrete gradients, Philosophical Transactions of the Royal Society of London. Series A: Mathematical, Physical and Engineering Sciences 357 (1754) (1999) 1021–1045. doi:10.1098/rsta.1999.0363.
- [15] L. W. Tu, An introduction to manifolds, Springer Science & Business Media, New York, NY, United States, 2010. doi:10.1007/978-1-4419-7400-6.
- [16] L. G. Taff, Celestial mechanics, Wiley, New York, NY, United States, 1985.
- [17] R. A. LaBudde, D. Greenspan, Discrete mechanics—a general treatment, Journal of Computational Physics 15 (2) (1974) 134–167. doi:10.1016/0021-9991(74)90081-3.
- [18] S. Kovalevskaya, Sur le problème de la rotation d’un corps solide autour d’un point fixe, Acta Mathematica 12 (1889) 177–232. doi:10.1007/BF02592182.
- [19] H. C. Öttinger, Beyond Equilibrium Thermodynamics, John Wiley & Sons, New York, NY, United States, 2005. doi:10.1002/0471727903.
- [20] F. Gay-Balmaz, H. Yoshimura, A Lagrangian variational formulation for nonequilibrium thermodynamics. Part I: Discrete systems, Journal of Geometry and Physics 111 (2017) 169–193. doi:10.1016/j.geomphys.2016.08.018.
- [21] H. C. Öttinger, GENERIC formulation of Boltzmann’s kinetic equation, Journal of Non-Equilibrium Thermodynamics 22 (4) (1997) 386–391. doi:10.1515/jnet.1997.22.4.386.
- [22] T. B. Benjamin, J. L. Bona, J. J. Mahony, Model equations for long waves in nonlinear dispersive systems, Philosophical Transactions of the Royal Society of London. Series A, Mathematical and Physical Sciences 272 (1220) (1997) 47–78. doi:10.1098/rsta.1972.0032.
- [23] M. J. Ablowitz, H. Segur, Solitons and the Inverse Scattering Transform, Vol. 4 of Studies in Applied and Numerical Mathematics, SIAM, Philadelphia, PA, United States, 1981. doi:10.1137/1.9781611970883.
- [24] A. Ern, J.-L. Guermond, Finite elements I: approximation and interpolation, Vol. 72 of Texts in Applied Mathematics, Springer International Publishing, Cham, Switzerland, 2021. doi:10.1007/978-3-030-56341-7.
- [25] D. A. Ham, P. H. J. Kelly, L. Mitchell, C. J. Cotter, R. C. Kirby, K. Sagiya, N. Bouziani, S. Vorderwuelbecke, T. J. Gregory, J. Betteridge, D. R. Shapero, R. W. Nixon-Hill, C. J. Ward, P. E. Farrell, P. D. Brubeck, I. Marsden, T. H. Gibson, M. Homolya, T. Sun, A. T. T. McRae, F. Luporini, A. Gregory, M. Lange, S. W. Funke, F. Rathgeber, G.-T. Bercea, G. R. Markall, Firedrake user manual, Imperial College London, University of Oxford, Baylor University, University of Washington (2023). doi:10.25561/104839.
- [26] S. Balay, S. Abhyankar, M. F. Adams, S. Benson, J. Brown, P. Brune, K. Buschelman, E. Constantinescu, L. Dalcin, A. Dener, V. Eijkhout, J. Faibussowitsch, W. D. Gropp, V. Hapla, T. Isaac, P. Jolivet, D. Karpeev, D. Kaushik, M. G. Knepley, F. Kong, S. Kruger, D. A. May, L. C. McInnes, R. T. Mills, L. Mitchell, T. Munson, J. E. Roman, K. Rupp, P. Sanan, J. Sarich, B. F. Smith, S. Zampini, H. Zhang, H. Zhang, J. Zhang, PETSc/TAO users manual, Argonne National Laboratory (ANL-21/39 - Revision 3.21) (2024). doi:10.2172/2205494.
- [27] P. R. Amestoy, I. S. Duff, J. Koster, J.-Y. L’Excellent, A fully asynchronous multifrontal solver using distributed dynamic scheduling, SIAM Journal on Matrix Analysis and Applications 23 (1) (2001) 15–41.

- [28] B. D. Andrews, P. E. Farrell, Software used in ‘Conservative and dissipative discretisations of multi-conservative ODEs and GENERIC systems’ (2025). doi : 10.5281/zenodo.17750373.